DEOXYGENATION OF PALM FATTY ACID DISTILLATE TO GREEN DIESEL OVER MOLYBDENUM NITRIDE AND CARBIDE-BASED CATALYSTS IN A TRICKLE-BED REACTOR

Miss Wanwipa Leangsiri

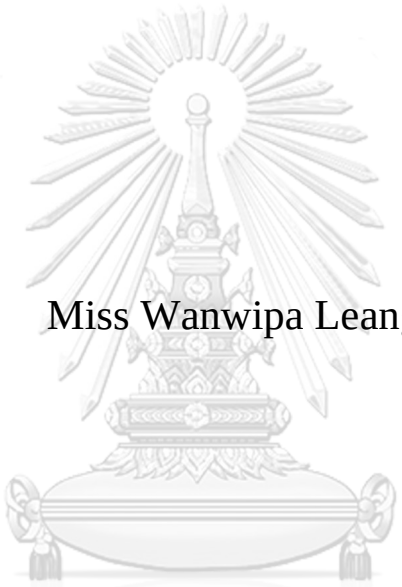

จุฬาลงกรณ์มหาวิทยาลัย
Chulalongkorn University

A Thesis Submitted in Partial Fulfillment of the Requirements
for the Degree of Master of Engineering in Chemical Engineering
Department of Chemical Engineering
FACULTY OF ENGINEERING
Chulalongkorn University
Academic Year 2020
Copyright of Chulalongkorn University

ดีออกซิจิเนชันของกรดไขมันปาล์มเพื่อผลิตกรีนดีเซลบนตัวเร่งปฏิกิริยาที่มีโมลิบดีนัมไนไตรด์และคาร์ไบด์เป็นหลักในเครื่องปฏิกรณ์แบบทริกเคิลเบด

น.ส.วัลวิภา เลี้ยงศิริ

จุฬาลงกรณ์มหาวิทยาลัย
CHULALONGKORN UNIVERSITY

วิทยานิพนธ์นี้เป็นส่วนหนึ่งของการศึกษาตามหลักสูตรปริญญาวิศวกรรมศาสตรมหาบัณฑิต
สาขาวิชาวิศวกรรมเคมี ภาควิชาวิศวกรรมเคมี
คณะวิศวกรรมศาสตร์ จุฬาลงกรณ์มหาวิทยาลัย
ปีการศึกษา 2563
ลิขสิทธิ์ของจุฬาลงกรณ์มหาวิทยาลัย

Thesis Title	DEOXYGENATION OF PALM FATTY ACID DISTILLATE TO GREEN DIESEL OVER MOLYBDENUM NITRIDE AND CARBIDE-BASED CATALYSTS IN A TRICKLE-BED REACTOR
By	Miss Wanwipa Leangsiri
Field of Study	Chemical Engineering
Thesis Advisor	Professor SUTTICHAI ASSABUMRUNGRAT
Thesis Co Advisor	Assistant Professor Worapon Kiatkittipong

Accepted by the FACULTY OF ENGINEERING, Chulalongkorn University in Partial Fulfillment of the Requirement for the Master of Engineering

..... Dean of the FACULTY OF ENGINEERING
(Professor SUPOT TEACHAVORASINSKUN)

THESIS COMMITTEE

..... Chairman
(Dr. AKAWAT SRIRISUK)

..... Thesis Advisor
(Professor SUTTICHAI ASSABUMRUNGRAT)

..... Thesis Co-Advisor
(Assistant Professor Worapon Kiatkittipong)

..... Examiner
(Assistant Professor PALANG BUMROONGSAKULSAWAT)

..... External Examiner
(Dr. Atthapon Srifa)

จุฬาลงกรณ์มหาวิทยาลัย
Chulalongkorn University

วัลวิภา เลี้ยงศิริ : ดีออกซิจิเนชันของกรดไขมันปาล์มเพื่อผลิตกรีนดีเซลบนตัวเร่งปฏิกิริยาที่มีโมลิบดีนัมไนไตรด์และคาร์ไบด์เป็นหลักในเครื่องปฏิกรณ์แบบทริกเคิลเบด . (DEOXYGENATION OF PALM FATTY ACID DISTILLATE TO GREEN DIESEL OVER MOLYBDENUM NITRIDE AND CARBIDE-BASED CATALYSTS IN A TRICKLE-BED REACTOR) อ.ที่ปรึกษาหลัก : ศ. ดร.สุทธิชัย อัสสะบำรุงรัตน์, อ.ที่ปรึกษาร่วม : ผศ. ดร.วรพล เกียรติกิตติพงษ์

ในงานวิจัยนี้ กรดไขมันปาล์มถูกดีออกซิจิเนชันเพื่อผลิตกรีนดีเซล โดยใช้ตัวเร่งปฏิกิริยาแกมม่าอลูมิน่าที่รองรับโลหะผสมโคบอลต์โมลิบดีนัมและนิกเกิลโมลิบดีนัมที่มีเฟสคาร์ไบด์และไนไตรด์ ในเครื่องปฏิกรณ์แบบทริกเคิลเบด ตัวเร่งปฏิกิริยาเตรียมขึ้นโดยวิธีการสลายตัวขั้นตอนเดียวของส่วนผสมเฮกซะเมทิลีนเตตรามีนและเกลือโลหะที่เกี่ยวข้อง โดยมีไฮโดรเจนและไนโตรเจนเพื่อรูปแบบคาร์ไบด์และไนไตรด์ตามลำดับที่อุณหภูมิ 700 องศาเซลเซียส ตัวเร่งปฏิกิริยาที่เตรียมขึ้นถูกวิเคราะห์ด้วยเทคนิค ดังนี้ เอกซ์เรย์ดิฟแฟรกชัน การถูกซับทางกายภาพด้วยแก๊สไนโตรเจน จุลทรรศน์อิเล็กตรอนแบบสแกนนิงและจุลวิเคราะห์ และการวิเคราะห์การเปลี่ยนแปลงน้ำหนักของตัวเร่งปฏิกิริยาเชิงอุณหภูมิความร้อน ประสิทธิภาพของตัวเร่งปฏิกิริยาได้รับการประเมินที่อุณหภูมิ 330 องศาเซลเซียส ความดันแก๊สไฮโดรเจน 5 เมกะปาสคาล อัตราการไหลของสารตั้งต้นต่อปริมาตรของตัวเร่งปฏิกิริยาเท่ากับ 1 ต่อชั่วโมง และอัตราส่วนระหว่างแก๊สไฮโดรเจนต่อสารตั้งต้นเท่ากับ 1000 ลบ.ซม.ต่อลบ.ซม. พบว่าตัวเร่งปฏิกิริยาคาร์ไบด์แสดงให้เห็นถึงประสิทธิภาพที่เหนือกว่าตัวเร่งปฏิกิริยาไนไตรด์ ตัวเร่งปฏิกิริยาโลหะผสมโคบอลต์โมลิบดีนัมมีอัตราการเลือกเกิดของผลิตภัณฑ์ดีเซลสูงกว่าโลหะเดี่ยวโมลิบดีนัมและโลหะผสมนิกเกิลโมลิบดีนัม ดังนั้นตัวเร่งปฏิกิริยาโคบอลต์โมลิบดีนัมและนิกเกิลโมลิบดีนัมคาร์ไบด์จึงถูกเลือกเพื่อทดสอบเพิ่มเติม ตัวเร่งปฏิกิริยาที่เตรียมโดยวิธีสลายตัวขั้นตอนเดียวสามารถเร่งปฏิกิริยาได้สูงกว่าวิธีการตั้งโปรแกรมอุณหภูมิ ซึ่งอาจเกิดจากพื้นที่ผิวของตัวเร่งปฏิกิริยาที่สูงกว่า เพื่อปรับสภาวะการทำงานให้เหมาะสม ได้ศึกษาในช่วงอุณหภูมิ 300-390 องศาเซลเซียส และความดันไฮโดรเจน 3-5 เมกะปาสคาล พบว่าอุณหภูมิในสภาวะการทำงานที่ 330 องศาเซลเซียส และความดันไฮโดรเจน 5 เมกะปาสคาล เป็นสภาวะที่เหมาะสมสำหรับตัวเร่งปฏิกิริยาโคบอลต์โมลิบดีนัมและนิกเกิลโมลิบดีนัมคาร์ไบด์ ในการทดสอบความเสถียร ตัวเร่งปฏิกิริยาโคบอลต์โมลิบดีนัมคาร์ไบด์แสดงค่าการเปลี่ยนแปลงกรดไขมันที่สมบูรณ์ โดยให้ค่าการเลือกเกิดของผลิตภัณฑ์ดีเซล 82% เป็นเวลาทำปฏิกิริยา 72 ชั่วโมง อย่างไรก็ตามกิจกรรมการเร่งปฏิกิริยาของโคบอลต์โมลิบดีนัมคาร์ไบด์ค่อยๆลดลงหลังจาก 72 ชั่วโมง โดยค่าการเปลี่ยนแปลงกรดไขมัน 81% และค่าการเลือกเกิดของผลิตภัณฑ์ดีเซล 68.5% หลังจากผ่านไป 102 ชั่วโมง

จุฬาลงกรณ์มหาวิทยาลัย
Chulalongkorn University

สาขาวิชา	วิศวกรรมเคมี	ลายมือชื่อนิสิต .....
ปีการศึกษา	2563	ลายมือชื่อ อ.ที่ปรึกษาหลัก .....
		ลายมือชื่อ อ.ที่ปรึกษาร่วม .....

6170269821 : MAJOR CHEMICAL ENGINEERING
KEYWORD: Green diesel, Bio-hydrogenated diesel, Hydrodeoxygenation, Deoxygenation, Palm fatty acid distillate, Transition metal carbides, Transition metal nitrides

Wanwipa Leangsiri : DEOXYGENATION OF PALM FATTY ACID DISTILLATE TO GREEN DIESEL OVER MOLYBDENUM NITRIDE AND CARBIDE-BASED CATALYSTS IN A TRICKLE-BED REACTOR. Advisor: Prof. SUTTICHAI ASSABUMRUNGRAT Co-advisor: Asst. Prof. Worapon Kiatkittipong

In this present work, the deoxygenation of palm fatty acid distillate (PFAD) to green diesel over γ-Al_2O_3 supported bimetallic CoMo and NiMo carbide and nitride catalysts was conducted in a trickle bed reactor. The catalysts were prepared by a single-step decomposition method of mixture containing hexamethylenetetramine and corresponding metal salts in presence of hydrogen and nitrogen for carbide and nitride forms, respectively at 700 ºC. The prepared catalysts were characterized by XRD, XPS, N_2-sorption, SEM/EDX and TGA techniques. The catalyst performance was evaluated at a temperature of 330 °C, hydrogen pressure of 5 MPa, LHSV of 1 h^{-1}, and H_2/feed ratio of 1000 N($cm^3 \cdot cm^{-3}$). It was found that the carbide catalysts exhibited the superior performance that those of nitride catalysts. The bimetallic CoMoC showed higher diesel yield than monometallic Mo carbide and bimetallic NiMoC catalysts. Thus, the CoMoC and NiMoC catalysts were selected for further investigations. The catalysts prepared by a single-step decomposition method exhibited higher catalytic activity than that of catalysts prepared by temperature-programmed reduction method due to higher catalyst surface area. In order to optimize the operating conditions, the operating temperatures were varied from 300 to 390 °C under 3-5 MPa of hydrogen pressure. The operating temperature of 330 °C and 5 MPa of hydrogen pressure was found to be a suitable condition for CoMoC and NiMoC catalysts. In the stability test, the CoMoC catalyst exhibited complete PFAD conversion with diesel yield 82.0% for 72 h. time on stream. However, the catalytic activity of CoMoC catalyst gradually decreased after 72 h. and PFAD conversion of 81% with diesel yield of 68.5% were obtained after 102 h. time on stream.

Field of Study:	Chemical Engineering	Student's Signature .....
Academic Year:	2020	Advisor's Signature .....
		Co-advisor's Signature .....

ACKNOWLEDGEMENTS

I would like to sincerely grateful for everyone contributing to the completion of my thesis. However, my appreciation extends to those whose names are not mentioned here.

First of all, I really appreciate and would like to express my sincere thankfulness to my thesis advisor, Prof. Suttichai Assabumrungrat and my co-advisor, Assist. Prof. Worapon Kiatkitipong for supervision, guidance, suggestions and continuous support throughout my research.

I would like to grateful to Dr. Akawat sririsuk as the chairman, Assist. Prof. Palang bumroongsakulsawat as a member of the thesis committee and Dr. Atthapon Srifa as a member of the external examiner, for their helpful comments and suggestions.

Moreover, I would like to grateful to the scientists, my seniors, my friend, who are the members of the Center of excellence on catalysis and catalytic reaction engineering, Chulalongkorn University and Catalytic reaction, Silpakorn University, for the assistance and support of my research.

จุฬาลงกรณ์มหาวิทยาลัย
Chulalongkorn University

Finally, I would give my deepest thanks to my family, who always supports, encourages, and understands.

Wanwipa Leangsiri

TABLE OF CONTENTS

Page

จุฬาลงกรณ์มหาวิทยาลัย
Chulalongkorn University

จุฬาลงกรณ์มหาวิทยาลัย
Chulalongkorn University

จุฬาลงกรณ์มหาวิทยาลัย
Chulalongkorn University

LIST OF TABLES

จุฬาลงกรณ์มหาวิทยาลัย
Chulalongkorn University

จุฬาลงกรณ์มหาวิทยาลัย
CHULALONGKORN UNIVERSITY

LIST OF FIGURES

จุฬาลงกรณ์มหาวิทยาลัย
Chulalongkorn University

จุฬาลงกรณ์มหาวิทยาลัย
Chulalongkorn University

LIST OF ABBREVIATIONS

ASTM	American society for testing and materials
BHD	bio-hydrogenated diesel
CoMoC/Al	$Co_3Mo_3C/\gamma\text{-}Al_2O_3$ catalyst
CoMoC/Al-TPR	$Co_3Mo_3C/\gamma\text{-}Al_2O_3$ catalyst prepare by the temperature-programmed reduction method
CoMoN/Al	$Co_3Mo_3N/\gamma\text{-}Al_2O_3$ catalyst
DCO	decarbonylation
DCO_2	decarboxylation
DCO_x	decarbonylation and decarboxylation
DTG	derivative thermogravimetry
FAME	fatty acid methyl ester
FFA	free fatty acid
HDO	hydrodeoxygenation
MoC/Al	$Mo_2C/\gamma\text{-}Al_2O_3$ catalyst
MoN/Al	$Mo_2N/\gamma\text{-}Al_2O_3$ catalyst
NiMoC/Al	$Ni_3Mo_3C/\gamma\text{-}Al_2O_3$ catalyst
NiMoC/Al-TPR	$Ni_3Mo_3C/\gamma\text{-}Al_2O_3$ catalyst prepare by the temperature-programmed reduction method
NiMoN/Al	$Ni_3Mo_3N/\gamma\text{-}Al_2O_3$ catalyst
PFAD	palm fatty acid distillate
TG	Triglyceride

จุฬาลงกรณ์มหาวิทยาลัย
CHULALONGKORN UNIVERSITY

CHAPTER I

INTRODUCTION

1.1 Introduction

The global warming problem is a trend to increase as the population increases. Increased CO_2 emissions are the main cause of global warming caused by human activities and many sectors. Transportation is a one of the sectors with the highest amount of CO_2 emission. These problems have many effects on our world both directly and indirectly [1]. As a result, many sectors have looked for the process to reduce CO_2 emission by improvement the clean fuel, so-called biofuel to replace fossil fuel by carbon-neutral cycle concept at the same time, the biofuel can be produced from biomass.

The biofuel was generated from biomass and their properties are similar to fossil fuel. Many plants have oil as the main component and can be used to produce fuel. There are many types of energy plants in Thailand such as palm oil, jatropha oil, soybean oil and rapeseed oil. In addition, waste cooking oil is a potential raw material to produce renewable fuels.

In the first-generation, many researchers are focusing on biofuel obtained from edible vegetable oil, animal fat or waste cooking oil by transesterification so called biodiesel (FAME) [2-4]. The food encroachment of humanity has resulted in efforts to find new biomass as a reactant of biofuel products. Biodiesel is a fuel that has oxygen content in molecules, which must be mixed with petroleum fuel to be used with diesel engines. The next generation of biofuel, bio-hydrogenated diesel or green diesel production via hydrotreating of waste cooking oil, nonedible vegetable oil and free fatty acid (FFA) [5-9]. Which has a structure like petroleum fuel, can be used instead of fuel without blend other fuels. In hydrotreating process, the free fatty acids can be used as a reactant instead of triglyceride for synthetic diesel production.

Palm fatty acid distillate (PFAD) is a by-product of refining crude palm oil which contains approximately 93.2% of free fatty acid including palmitic acid, oleic acid and linoleic acid [10]. Palm fatty acid distillate is a potential feedstock for producing green diesel *via* hydrodeoxygenation.

Sulfide NiMo/γ-Al_2O_3 catalysts and Pd/C are the commercial catalysts to produce green diesel, which are highly effective and have been studied in many research [11-14]. On the other hand, the sulfur content of sulfide NiMo/γ-Al_2O_3 catalyst in the product resulted in increase in purification costs in addition to cause an

air pollution by emission of SO_x. Therefore, this research aims to develop non-sulfide catalysts from transition metals in carbide and nitride forms.

1.2 Objectives of research

To develop nickel and cobalt promoted molybdenum nitride and carbide catalysts for deoxygenation of palm fatty acid distillate to green diesel in a trickle bed reactor.

1.3 Scope of Research

1.3.1. The transition carbide and nitride catalyst (MoC/Al, MoN/Al, CoMoC/Al, CoMoN/Al, NiMoC/Al and NiMoN/Al) were prepared by a single-step decomposition method in compared with conventional temperature-programmed reduction (TPR) method.

1.3.2. The synthesized catalysts were characterized XRD, XPS, N_2 sorption, SEM/EDX and TGA analysis. and liquid products were analyzed by CHNO/S analyzer, FT-IR and gas chromatography equipped with a flame ionization detector (FID). The compositions of gas products were analyzed by gas chromatography equipped with a thermal conductivity detector (TCD).

1.3.3. The catalyst performance was evaluated in a trickle-bed reactor under 330 ºC of temperature, 5 MPa of hydrogen pressure, 1 h^{-1} of LHSV and 1000 N($cm^3 \cdot cm^{-3}$) of H_2/feed ratio.

จุฬาลงกรณ์มหาวิทยาลัย
Chulalongkorn University

1.3.4. The catalytic activities of bimetallic carbide catalysts (CoMoC/Al and NiMoC/Al) prepared by a single-step decomposition method were compared with the catalysts prepared by conventional temperature-programmed reduction (TPR) method.

1.3.5. The reaction parameters for green diesel using the excellent catalysts under temperature (300-390 ºC) and hydrogen pressure (3-5 MPa) were optimized.

1.3.6. The stability of the excellent catalysts was evaluated *via* hydrotreating of palm fatty acid distillate (PFAD) under optimal conditions.

1.4 Research methodology

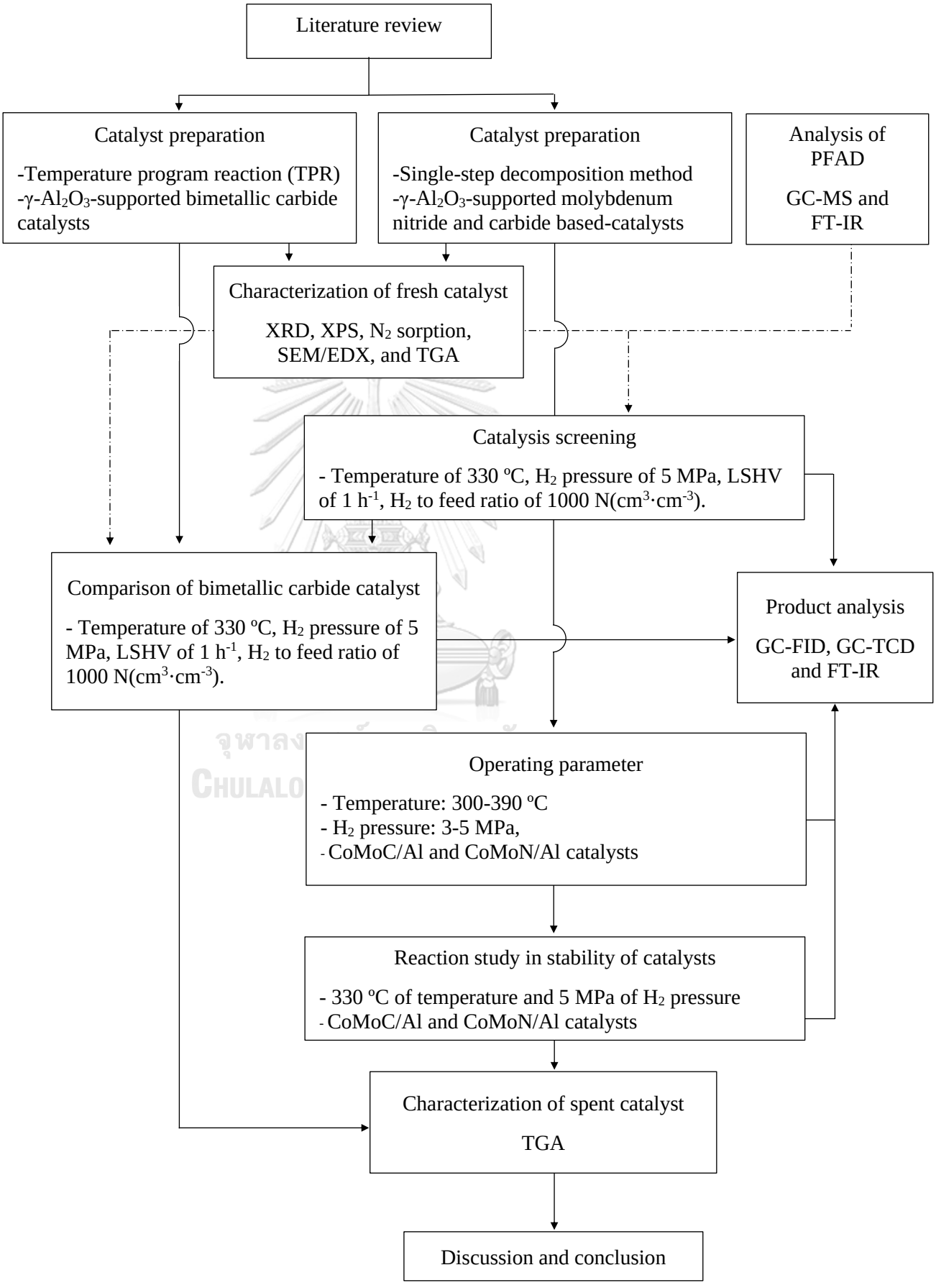

CHAPTER II

THEORY

2.1 Palm fatty acid distillate (PFAD)

Palm fatty acid distillate (PFAD) is a by-product of the physical refining process of crude palm oil. The physical refining process of crude palm oil is shown in Figure 1. palm fatty acid distillate (PFAD) in crude palm oil (COP) consists of about 4-5% by the refining palm oil process, which is separated from the deodorization process.

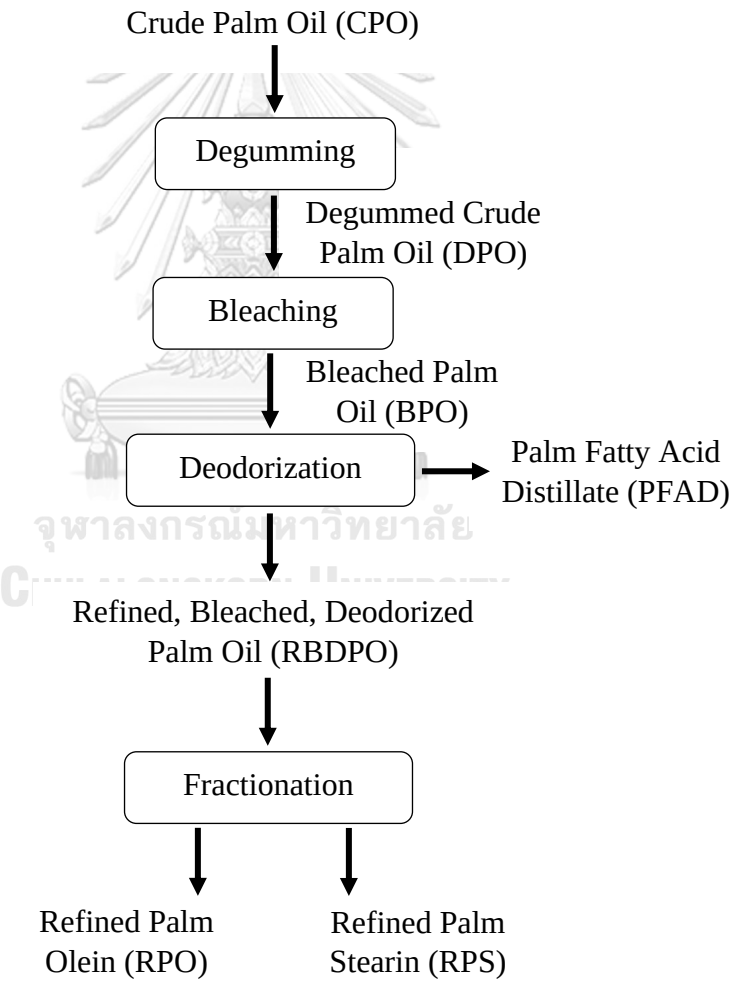

Figure 1 Physical refining process of crude palm oil [15].

Palm fatty acid distillate (PFAD) is a potential feedstock to produce a new generation of biofuel. Palm fatty acid distillate (PFAD) consists of 93.2 wt % FFA that mainly contains 49.0% palmitic acid, 35.8% oleic acid, and 8.3% linoleic acid with a small amount of other fatty acids and triglycerides, as shown in Table 1. Palm fatty acid distillate (PFAD) is a light brown solid at room temperature, which melts into a brown liquid at temperatures between 60 to 70 ºC [16].

Table 1 Composition of FFA in PFAD [10].

Fatty acid	**Wt. %**
C14:0 (myristic acid)	1.1
C16:0 (palmitic acid)	49.0
C16:1 (palmitoleic acid)	0.2
C18:0 (steric acid)	4.1
C18:1 (oleic acid)	35.8
C18:2 (linoleic acid)	8.3
C18:3 (linolenic acid)	0.3
C20:0 (arachidic acid)	0.3
C20:1 (eicosenoic acid)	0.2
C24:1 (tetracosenoic acid)	0.6

จุฬาลงกรณ์มหาวิทยาลัย
Chulalongkorn University

2.2 Hydrotreating process

The hydrotreating process can be converted triglyceride to n-alkane and iso-alkane at high temperature and high hydrogen pressure. First, the double bonds in the saturated molecule of triglycerides were hydrogenated to the unsaturated molecule of triglycerides, after that cracked to free fatty acid and propane. The free fatty acid eliminates oxygen content in molecules through three main reaction pathways for deoxygenation of free fatty acid to green diesel fuel generally consists of hydrodeoxygenation (HDO), decarbonylation (DCO) and decarboxylation (DCO_2), as shown in Figure 2. The other possible reaction occurs in the hydrotreating process revers water gas shift and methanation reaction are shown in Figure 3. The thermodynamic data of deoxygenation reaction and other possible reaction was shown in Table 2.

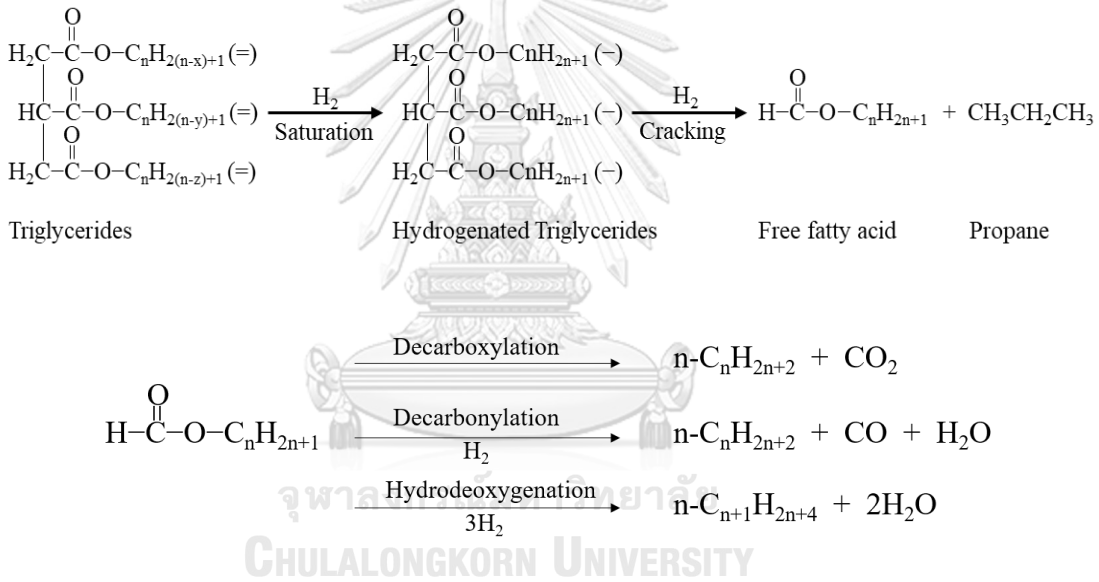

Figure 2 Reaction pathways for deoxygenation reaction of triglycerides to green diesel [17].

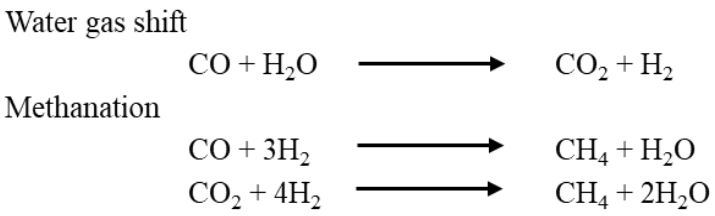

Figure 3 The other possible reaction occurs in the deoxygenation reaction [18, 19].

Table 2 The thermodynamic data of deoxygenation reaction and other possible reaction [19].

Liquid phase	**Reaction**	**ΔG^{o}_{533} (kJ mol^{-1})**	**ΔH^{o}_{533} (kJ mol^{-1})**
Hydrodeoxygenation	$R\text{-}COOH + 3H_2 \longrightarrow R\text{-}CH_3 + 2H_2O$	-88.0	-112.6
Decarbonylation	$R\text{-}COOH + H_2 \longrightarrow R\text{-}H + CO + H_2O$	-59.5	49.7
Decarboxylation	$R\text{-}COOH \longrightarrow R\text{-}H + CO_2$	-78.6	10.1
Gas phase	**Reaction**	**ΔG^{o}_{533} (kJ mol^{-1})**	**ΔH^{o}_{533} (kJ mol^{-1})**
Methanation	$CO + 3H_2 \longrightarrow CH_4 + H_2O$	-88.4	-215.3
Methanation	$CO2 + 4H_2 \longrightarrow CH_4 + 2H_2O$	-69.2	-175.7
Water gas shift	$CO + H_2O \longrightarrow CO_2 + H_2$	-19.1	-39.6

2.2.1 Hydrodeoxygenation (HDO)

Hydrodeoxygenation (HDO), an exothermic reaction, converts free fatty acid to n-alkane, which the same carbon number of free fatty acid and removes oxygen of free fatty acid in the form of water as a by-product.

2.2.2 Decarboxylation (DCO_2)

Decarboxylation (DCO_2), an endothermic reaction, convert the carboxyl groups in free fatty acid to n-alkane. Reaction pathway of free fatty acid to n-alkane are shown in Figure 4. First, the H-O bond cleaved to hydrogen ions and the carboxylate anions. Next, the carboxylate anion break to alkyl anions and carbon dioxide, which the carbon atom of free fatty acid loses to CO_2 (as a by-product). Finally, the alkyl anions react with H^+ to generate n-alkane. Therefore, the carbon number of a product by decarboxylation reaction reduces one number.

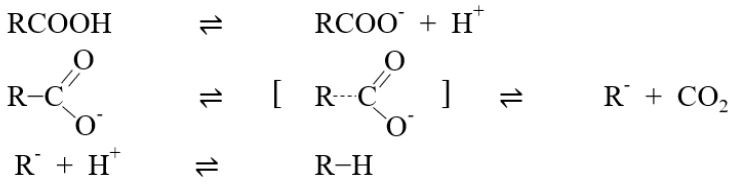

Figure 4 The reaction mechanism of free fatty acid to n-alkane [18].

2.2.3 Decarbonylation (DCO)

Decarbonylation (DCO), an endothermic reaction, comprise of two possible reaction pathways: (1) fatty acids are broken in the C–C bond, and then combine with H to give unsaturated straight-chain alkanes and lose acyl in form of CO. (2) saturated straight-chain alkanes and formic acid occur by direct hydrogenated of free fatty acid, then formic acid rapid decomposition to CO and H_2O as a byproduct. Therefore, the carbon number of a product by both decarbonylation reaction reduces to one number. The direct hydrogenate of free fatty acid to saturated straight-chain alkanes and decomposition of formic acid shown in Figure 5.

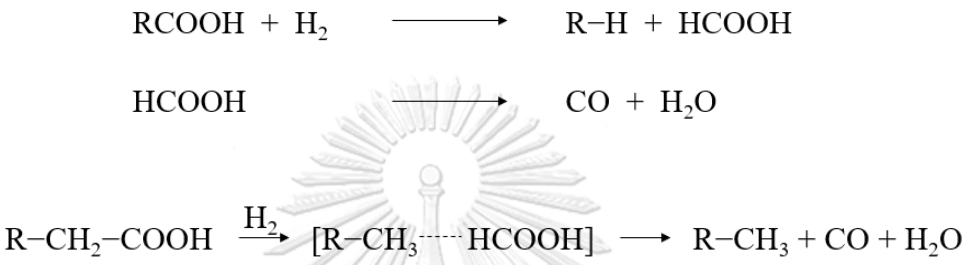

Figure 5 The reaction mechanism of free fatty acid to n-alkane by Decarbonylation [18, 20].

2.2.4 Isomerization and cracking

The n-alkane can be isomerization and cracking to produce iso-alkane and light hydrocarbon at the high reaction temperature, respectively. The n-alkane have a high cetane number, which good green diesel fuel properties. Therefore, isomerization and cracking reactions of n-alkane should be minimized [21]. On the other hand, the high amount of n-alkanes in green diesel fuel may also increase the cloud point and viscosity, and isomerization of the n-alkane may be desired [22].

2.2.5 Revers water-gas shift and Methanation reaction

Carbon dioxide, carbon monoxide and hydrogen are gas products by deoxygenation of free fatty acid to green diesel. Methane and water occur by methanation of carbon monoxide and hydrogen. Carbon monoxide reacts with water to produce carbon dioxide and hydrogen via a reverse water-gas shift.

2.2 Green diesel

Green diesel is renewable energy from biomass through a chemical process, which are also known as an organic liquid product. Green diesel are suitable for replacing petroleum diesel because it reduces CO_2 emissions and has properties similar to petroleum diesel. While petroleum diesel has sulfur and impurity content, are produce NOK (SO_x and NO_x), which are air pollution, when combustion in diesel engines. In addition, hydrodesulfurization (HDS) as a sulfur removal unit are expensive cost. Including, when biodiesel as a first-generation biofuel compares with green diesel. Biodiesel has oxygen content in the molecule so it must blend with petroleum diesel before used for diesel engines. Because biodiesel quality depends on feedstock for biodiesel production, a high degree of unsaturation makes a melting point lower causes high vulnerability to oxidation [23]. Table 3 shown comparing the properties of petroleum fuel and biofuel in both generations. The property of green diesel fuel closed to petroleum diesel fuel. ASTM International's standard and European diesel fuel standard (EN) are shown in Table 4.

จุฬาลงกรณ์มหาวิทยาลัย
Chulalongkorn University

Table 3 The physicochemical properties of diesel specification, biodiesel and green diesel [24, 25].

Parameter	EURO-IV Diesel specifications	FAME (Biodiesel)	BHD (Green diesel)
Density (kg m^{-3})	820-840	881	780
Viscosity at 40 (ºC)	2.0-4.5	4.41	2.5-3.5
Flash point, min (ºC)	35-66	168	120-138
Pour point, max (ºC)	3.0-15.0	5	9
Cloud point (ºC)	-5	1	-15 to -30
Calorific value (MJ kg^{-1})	-	37.98	44
Cetane number, min	51	50.8	80-90
Acid number (mg KOH g^{-1})	-	0.43	33.3
Sulphur content, max (mg kg^{-1})	50	20	< detection limit
Oxygen content (Wt.%)	-	12.8	-
Distillation (ºC)	-	394	265-320
Lubricity (HFRR), max. (μm)	460		360
Heating value (MJ kg)	43	38	44

จุฬาลงกรณ์มหาวิทยาลัย
Chulalongkorn University

Table 4 The standard test physical and chemical property of an organic liquid product [26, 27].

Properties	Unit	Method	
		European diesel fuel standard (EN)	**ASTM**
Density (15 ºC)	kg m^{-3}	EN ISO 3675, EN ISO 12185	ASTM D-4052
Viscosity (45 ºC)	mm^2 s^{-1}	EN ISO 3140	ASTM D-445
Fractional composition	ºC	EN ISO 3405	
Flash point	ºC		ASTM D-93
Cloud point	ºC		ASTM D-2500
Pour point	ºC		ASTM D-97, D-5297
Cetane index	-		ASTM D-4737
Corrosion	-		ASTM D-130
Color	-		ASTM D-1500
Thermal stability	% Reflectance		ASTM D-6468
Distillation	ºC		ASTM D86
Sulfur content	weight %		ASTM D-4294, D-5453
Aromatics	vol.%		ASTM D-1319
Total acid number (TAN)	mgKOH g^{-1}		ASTM D-664

จุฬาลงกรณ์มหาวิทยาลัย
Chulalongkorn University

CHAPTER III

LITERATURE REVIEWS

3.1 Feed for green diesel

Vegetable oil are an interesting source for green diesel production due to the mainly carbon atom in a range of the C_{12}-C_{18}, which is suitable for green diesel [28]. Vegetable oils contain triglycerides and free fatty acids, which triglyceride requires hydrogen consumption more than free fatty acids. Triglyceride needs to hydrogenate to free fatty acid and propane before deoxygenation reaction [17]. The free fatty acids are a potential raw material that is sustainable to produce green diesel because of low hydrogen consumption. hydrogen is an important raw material for green diesel production and expensive. In recent years, many studies have used free fatty acids, residues from the vegetable oil industry or model compounds, as raw materials instead of edible oil [29-37].

3.2 Sulfide catalysts

Sulfide catalysts are commercial catalysts in deoxygenation for green diesel. In industrial, sulfide catalysts are of importance to remove the sulfur and nitrogen from petroleum. The sulfide form of catalyst had a remarkable effect on deoxygenation reactions. Normally, molybdenum or tungsten is used as a major ingredient and nickel or cobalt.

Srifah et al. [38] studied the deoxygenation of palm oil for bio-hydrogenated diesel by $NiMoS_2/\gamma$-Al_2O_3 catalyst in a continuous fixed-bed reactor. This research varied conditions of 270-420 °C, 15-80 bar, 0.25-5.0 h^{-1} and hydrogen to oil ratio of 250-2000 N(cm^3 cm^{-3}). The results showed the product yield of 90.0% with 300 ºC of temperature, 30-50 bar of hydrogen pressure, 1.0-2.0 h^{-1} of LSHV and 750-1000 of hydrogen to oil ratio. The increased temperature from 300 ºC to 420 ºC with a decrease in product yield from 89.8% to 37.9% because of the promotion of isomerization, cracking, and cyclization. Higher pressure promoted HDO reaction while the increases in LHSV suppressed reactions due to insufficient contact time. Furthermore, methanation reaction impacted on hydrogen consumption at low temperature and high pressure. Furthermore, low temperature and high pressure impacted on hydrogen consumption with methanation reaction.

Yang et al. [39] studied biofuel production via Hydrotreating of C_{18} fatty acids over commercial sulfide Ni-W supported on modified SiO_2-Al_2O_3 by NTY zeolite catalyst, which dodecane as a solvent in a fixed bed reactor. Interested, the effects of operating conditions are temperature 300-375 °C, pressure 2-8 MPa, WHSV 4-18 h^{-1} and hydrogen to oil ratio 500-1000 N(mL mL^{-1}). The results showed temperature increasing with decreases the amount of diesel fraction while the total isomerization ratio increases because higher temperature promotes cracking reactions and restraints hydrogenation reactions. Low WHSV would promote cracking reactions causes to reduce the C_{15}-C_{18} yield and the isomerization ratio of the diesel fraction. High pressure and low C_{18} fatty acids concentration would promote the HDO while restraining the DCO/DCO_2 reactions due to the high ratio of adsorbed hydrogen to adsorbed C_{18} fatty acids molecules.

Toba et al. [40] studied the hydrodeoxygenation (HDO) of waste cooking oil over sulfide NiMo/Al_2O_3, CoMo/Al_2O_3 and NiW/Al_2O_3 catalysts were to produce high-quality transportation fuel. The result shows all sulfide catalysts showed high HDO activity and all waste oils gave n-paraffins, iso-paraffins and a small amount of olefins. NiMo and NiW catalysts showed high and stable hydrogenation activity, whereas the deactivation of hydrogenation activity was observed using CoMo catalyst. NiW catalyst promoted decarboxylation or decarbonylation than NiMo and CoMo catalysts. NiMo and NiW catalysts are more suitable for hydrodeoxygenation of low-grade waste oils than CoMo catalyst to prevent the formation of olefin. Sulfur eliminated from the sulfide catalyst and dissolved into a product at the initial stage of the reaction, while sulfur content of the product was low when catalytic activity showed constantly.

จุฬาลงกรณ์มหาวิทยาลัย
Chulalongkorn University

3.3 Noble metal and metal catalysts

Srifah et al. [41] studied the green diesel production via the hydrodeoxygenation of palm olein using monometallic catalysts (Co, Ni, Pd, and Pt) on γ-Al_2O_3 in a continuous trickle-bed reactor under the conditions are 270-420 °C of temperature, 15-80 bar of hydrogen pressure, 0.25-5.0 h^{-1} of LSHV, and 250-2000 N(cm^3 cm^{-3}) of hydrogen to oil ratio. The catalysts with various metal loadings (2–10 wt.%). The result showed the catalyst activity decreased in the order of product yield Co > Pd > Pt > Ni, compared at the same amount of metal loading. The Ni, Pd and Pt catalyst on γ-Al_2O_3 promoted decarbonylation reaction more than hydrodeoxygenation reaction. Simultaneously, the Co/γ-Al_2O_3 catalyst was nearly comparable between decarbonylation and/or decarboxylation with hydrodeoxygenation reaction. The reaction network of the model compound and oleic acid over the Ni, Co, Pd and Pt catalyst on γ-Al_2O_3 shown in Figure 6.

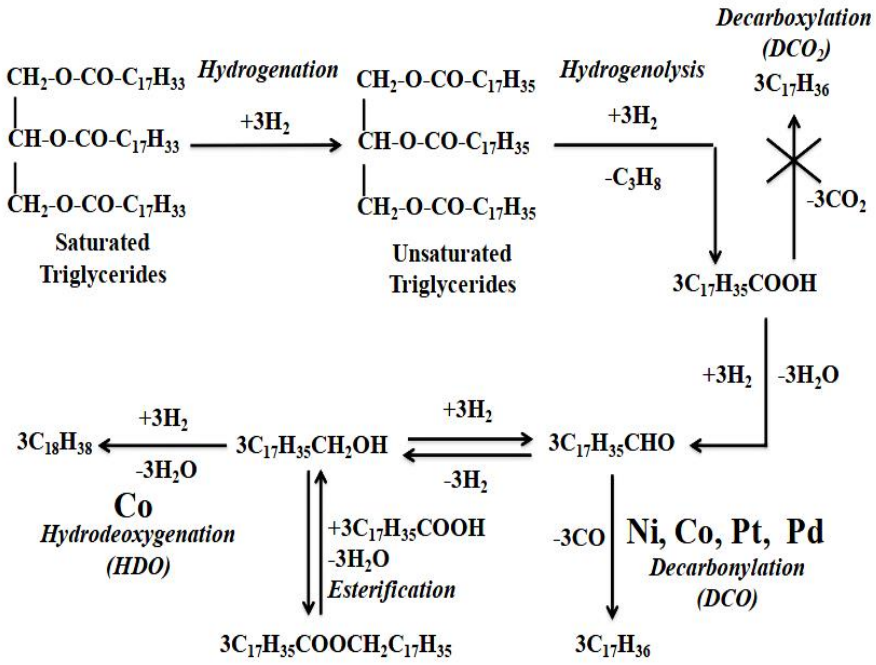

Figure 6 The reaction network of Ni, Co, Pd and Pt catalyst on γ-Al_2O_3 [41].

Snåre et al. [42] studied the screening of metal catalysts (Pd, Pt, Ru, Mo, Ni, Rh, Ir, and Os) supported on carbon, Al_2O_3, and SiO_2 for production of diesel-like hydrocarbons via catalytic deoxygenation of stearic acid in a semi-batch reactor. The condition was constant at 300 ºC of temperature and 6 bars of hydrogen pressure. The catalysts screening results show highly active and selective in the deoxygenation of the reaction of palladium catalysts on carbon-supported, which converted stearic acid completely with > 98% selectivity toward deoxygenated C_{17} products. The outcome of comparison with different metals on the equivalent supports by same metal content that the beneficial effect of metal in the deoxygenation reaction is in the descending order Pd > Pt > Ni > Rh > Ir > Ru > Os catalysts. Furthermore, the decarboxylation reaction was more radical over the Pd/C catalyst, while the decarbonylation reaction was more apparent over the Pt/C catalyst.

3.4 Metal carbides, metal nitrides and metal phosphides catalysts

Phimsen et al. [13] studied the effect of nickel catalysts i.e. nickel sulfide (NiS), nickel phosphide (NiP) and nickel carbide (NiC) was investigated for hydrotreating of spent coffee oil to produce bio-hydrotreated fuel (BHF). The condition of hydrotreating was performed at a 375-425 °C, 20-40 bar of initial H_2 pressure (before heating) with a reaction time of 0–3 h. The activity of the catalysts decreases in the order of NiC > NiP > NiS. NiC tended to promote the cracking reaction, which high gasoline and gaseous yields. The decarbonylation (DCO) more than decarboxylation (DCO_2) and hydrodeoxygenation (HDO) for deoxygenation of coffee oil for all the catalysts. The (DCO + DCO_2) to HDO ratio decreased in the order NiS > NiC > NiP. Straight-chain hydrocarbons are the main products, which high cetane index (> 110).

Monnier et al. [43] studied hydrodeoxygenation of oleic acid and canola oil by molybdenum, tungsten and vanadium supported on γ-Al_2O_3 were prepared by the temperature-programmed reaction. The condition of hydrodeoxygenation is performed at 380-410 ºC and 7.15 MPa of hydrogen pressure. The result showed the molybdenum nitride catalyst high catalytic hydrotreating of oleic acid (in terms of fatty acid conversion, oxygen removal and production of normal alkanes) more than to the vanadium and tungsten nitrides catalyst. The dominant reaction pathways of γ-Al_2O_3 supported molybdenum catalyst are hydrodeoxygenation while the decarbonylation and decarboxylation promoted to hydrocarbon of γ-Al_2O_3 supported vanadium nitride catalyst. A 450 h hydrotreating test performed at 400 ºC and 8.35 MPa hydrogen pressure of canola oil with Mo_2N/γ-Al_2O_3 catalyst indicated high oxygen removal throughout the test, which exceeds 90%.

จุฬาลงกรณ์มหาวิทยาลัย
Chulalongkorn University

Stefan et al. [36] studied the hydrodeoxygenation of oleic acid comparison between carbon nanofiber supported W_2C and Mo_2C catalysts. This research investigated activity, selectivity, and stability to evaluate the catalytic potential for the upgrading of fat/oil feeds. W_2C/CNF catalyst was more selective toward olefins, whereas Mo_2C/CNF catalyst was more selective toward paraffins. Mo_2C/CNF catalyst showed higher activity and stability compared with W_2C/CNF catalyst. The metal carbide catalyst promoted hydrodeoxygenation of unsaturated fatty acids. The olefinic products of W_2C/CNF catalyst higher than Mo_2C/CNF catalyst, which resulted in a higher deactivation rate of the tungsten-based catalyst. In addition, W_2C/CNF catalyst presented more sensitivity to oxidation compared with Mo_2C/CNF catalyst. W_2C/CNF catalyst is shown more suitable for production as a high value olefinic product. on the other hand, Mo_2C/CNF catalyst shows increased activity and catalyst stability more than Mo_2C/CNF catalyst.

Wang et al. [44] studied the diesel-like hydrocarbons production via the hydrotreatment of fatty acids using activated carbon-supported Mo_2C and W_2C catalysts under 360 °C of temperature, 3.0 MPa of hydrogen pressure and 3.0 h of reaction time. The result showed that high carburization temperature was feasible for W_2C/AC catalyst, but not for Mo_2C/AC catalyst because it resulted in an agglomeration of molybdenum compound and destruction of catalyst. The high reaction temperature highly improved the conversion over Mo_2C/AC catalyst and W_2C/AC catalyst during hydrotreatment of fatty acid. The conversion of Mo_2C/AC catalyst prepared at 700 °C and W_2C/AC catalyst prepared at 900 °C are 96.01% and 54.88%, respectively. The 20% loading of both Mo_2C/AC catalyst and W_2C/AC catalyst are the best metal loading due to high active sites and low agglomeration. Moreover, the high temperature promoted the cracking degree and DCO route. The proposed pathway of the hydrotreatment reaction of fatty acids to green diesel is shown in Figure 7.

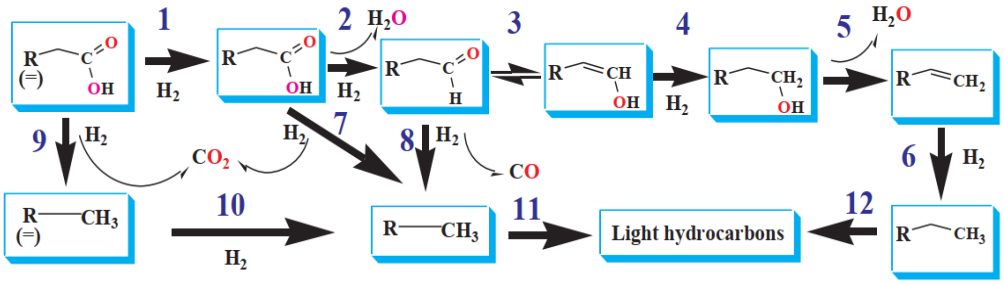

Figure 7 The proposed pathway of the hydrotreatment reaction of fatty acids to green diesel [44].

จุฬาลงกรณ์มหาวิทยาลัย
CHULALONGKORN UNIVERSITY

Phimsen et al. [45] studied the nickel-based carbide catalysts combined with Mo, Nb, W, and Zr on Al-SBA-15 support were investigated for the hydrocracking of distillers dried grains with soluble (DDGS) corn oil to produce biofuels under 400 ºC of temperature and 4.48 MPa of hydrogen pressure. Interested, the effects of the fractional sums of the electronegativities of the transition metals on the catalyst activities, selectivity and liabilities. NiWC/Al-SBA-15 catalyst highest diesel selectivity with a fractional sum of electronegativity of 2.06. The NiNbC/Al-SBA-15 catalyst promoted with 5% Ce maintained stable activity for 168 h at 400 ºC and 4.48 MPa hydrogen pressure. Adding Ce adjusting the combined electronegativities nearer to 2.0-2.2, which improved catalyst performance. On the other hand, adding Ce effected to textural properties, or the performance of individual metals could also impact catalyst performance.

As a summary, various oil sources, various non-sulfide catalysts type, reactor type, reaction condition, main product by hydrotreating are shown in Table 5.

จุฬาลงกรณ์มหาวิทยาลัย
Chulalongkorn University

Table 5 The various non-sulfide catalyst type and reaction conditions of hydrotreating for product biofuel.

Item	Catalyst	Oil	Reactor	Condition	Main product	Performance	Ref.
1	Mo_2C/RGO	Oleic acid	Fixed bed reactor	T=350 ºC P=5 MPa LSHV=2 h^{-1} H_2/oil ratio = 4.5 N($cm^3 \cdot cm^{-3}$)	C_{17}-C_{18} Hydrocarbon	Selectivity: 90 % Yield: 84.5 %	[46]
	Mo_2C/AC					Selectivity: 60 % Yield: 50.3 %	
2	Mo_2C/RGO	Soybean oil	Fixed bed reactor	T=350 ºC P=5 MPa LSHV=2 h^{-1} H_2/oil ratio = 30 N($cm^3 \cdot cm^{-3}$)	C_{17}-C_{18} Hydrocarbon	Selectivity: 72 % Yield: 45.7 %	[46]

จุฬาลงกรณ์มหาวิทยาลัย Chulalongkorn University

Table 6 The various non-sulfide catalyst type and reaction conditions of hydrotreating for product biofuel.

Item	Catalyst	Oil	Reactor	Condition	Main product	Performance	Ref.
3	$Mo_2N/\gamma Al_2O_3$	Oleic acid	Continuous flow microreactor	T=380 ºC P=7.15 MPa LSHV=0.45 h^{-1} H_2/oil ratio = 810 N($cm^3 \cdot cm^{-3}$)	C_{18} n-alkane	Conversion: 100 % Yield: 84.1 %	[43]
	$VN/\gamma Al_2O_3$					Conversion: 97 % Yield: 85 %	
	$WN/\gamma Al_2O_3$					Conversion: 97 % Yield: 81.1 %	
4	Mo_2C/AC	Palmitic acid and Oleic acid	Batch reactor	T=360 ºC P=3 MPa Reaction=3 h	C_{15}-C_{18} n-alkane	Conversion: 96 % Yield: 82.3 %	[44]
	W_2C/AC					Conversion: 55 % Yield: 51.6 %	
5	$NiMo/\gamma$-Al_2O_3	Rubber seed oil	Fixed bed tubular reactor	T=350 ºC P=3.5 MPa WSHV=1 h^{-1} H_2/oil ratio = 1000 N($cm^3 \cdot cm^{-3}$)	C_{15}-C_{18} n-alkane	Conversion: 99 % Yield: 80.9 %	[14]

Table 7 The various non-sulfide catalyst type and reaction conditions of hydrotreating for product biofuel.

Item	Catalyst	Oil	Reactor	Condition	Main product	Performance	Ref.
6	NiC/γ-Al_2O_3	Spent coffee oil	Batch reactor	T=400 ºC Initial H_2 P=4 MPa Reaction=2 h	C_5-C_{11} and C_{12}-C_{18} n-alkane	Conversion: 79 % Yield: 65.3 wt%	[13]
	NiP/γ-Al_2O_3					Conversion: 77 % Yield: 65.0 wt%	
7	NiMoC/Al-SBA-15	Soybean oils	Fixed bed reactor	T=400 ºC P=4.48 MPa LSHV=1 h^{-1} H_2 flow rate 50 ml min^{-1}	C_{15}-C_{18} n-alkane	Conversion: 100 % Selectivity: 97wt%	[47]
	NiMoC/γ-Al_2O_3					Conversion: 100 % Selectivity: 76wt%	
	NiMoC/USY					Conversion: 100 % Selectivity: 54wt%	

จุฬาลงกรณ์มหาวิทยาลัย
Chulalongkorn University

CHAPTER IV

METHODOLOGY

4.1 Chemicals

Table 6 lists the chemicals used in this study.

Table 8 The details of chemicals used in this study

Chemicals	Formula	Purity	Manufacture
PFAD	-	-	Patum Vegetable Thailand
Ammonium molybdate	$(NH_4)_6Mo_7O_{24}{\cdot}4H_2O$	81.0-83.0%	UNILAB
Nickel nitrate	$Ni(NO_3)_2{\cdot}6H_2O$	97.0%	UNILAB
Cobalt nitrate	$Co(NO_3)_2 \cdot 6H_2O$	100%	Ajax Finechem
Hexamethylenetetramine	$C_6H_{12}N_4$	99.0%	Sigma Aldrich
Ammonia solution	NH_4OH	25%	ChemX
Aluminum oxide	γ-Al_2O_3	Assay 100%	Fluka
Hydrogen gas	H_2	99.9%	Linde
Nitrogen gas	N_2	99.9%	Linde

จุฬาลงกรณ์มหาวิทยาลัย
Chulalongkorn University

4.2 Catalyst preparation

4.2.1 Preparation of molybdenum nitride and carbide-based catalysts on γ-Al_2O_3 support by the single-step decomposition method

The γ-Al_2O_3 support was crushed and sieved to 0.45-1.00 mm particle size for all catalysts. A mixture for the Mo_2N and Mo_2C supported on γ-Al_2O_3 catalysts were prepared by dissolving hexamethylenetetramine (HMTA) and ammonium heptamolybdate ($(NH_4)_6Mo_7O_{24}\cdot 4H_2O$) with a fixed molar ratio of 1:2, and a proper amount of γ-Al_2O_3 in 15% ammonia solution. The solution was stirred for 24 h. at room temperature. The molybdenum content was fixed 20% by weight. In the case of bimetallic catalysts, the Mo_3Ni_3N, Mo_3Ni_3C, Mo_3Co_3N and Mo_3Co_3C supported on γ-Al_2O_3 catalysts were prepared by dissolving ammonium heptamolybdate ($(NH_4)_6Mo_7O_{24}\cdot 4H_2O$), Nickel nitrate ($Ni(NO_3)_2\cdot 6H_2O$) or Cobalt nitrate ($Co(NO_3)_2 \cdot 6H_2O$) and hexamethylenetetramine (HMTA) with a fixed molar ratio of 2:14:34, and a proper amount of γ-Al_2O_3 in 15% ammonia solution. The solution was stirred for 24 h. at room temperature. The metal content was fixed 20% by weight. Then Ni_3Mo_3X and Co_3Mo_3X support on γ-Al_2O_3 by were prepared by impregnation method. After impregnation, all catalysts were dried for an overnight at 120°C. The resultant samples were activated under flowing nitrogen (nitride forms) and hydrogen (carbide forms) at a heating rate of 3 ºC min^{-1} to 700 ºC for 3 h. Finally, the carbide and nitride catalysts were cooled to room temperature in nitrogen and hydrogen, respectively.

4.2.2 Preparation of molybdenum carbide-based catalysts by temperature-programmed reduction (TPR) method

จุฬาลงกรณ์มหาวิทยาลัย
Chulalongkorn University

The γ-Al_2O_3 support was crushed and sieved to 0.45-1.0 mm particle size for all catalysts. The γ-Al_2O_3 supported Ni_3Mo_3C and Co_3Mo_3C catalysts were prepared by co-impregnation. First, NiMo and CoMo were supported on γ-Al_2O_3 by impregnating of an aqueous solution of ammonium heptamolybdate ($(NH_4)_6Mo_7O_{24}\cdot 4H_2O$) and Nickel nitrate ($Ni(NO_3)_2\cdot 6H_2O$) or Cobalt nitrate ($Co(NO_3)_2\cdot 6H_2O$). Then, the sample was dried overnight at 120 ºC and calcined at 500 ºC for 5 h. to obtain the γ-Al_2O_3 supported metal oxide catalysts with the metal loading of 20 wt.%. The resultant samples were activated under 20%CH_4/H_2 at a heating rate of 10 ºC min^{-1} to 250 ºC, then heated up to 700 ºC for half an hour to obtain Ni_3Mo_3C/γ-Al_2O_3 and Co_3Mo_3C/γ-Al_2O_3 catalysts. Finally, the supported bimetallic carbide catalysts were cooled to room temperature.

4.3 Catalyst characterizations

4.3.1 X-ray diffraction

The crystal structure and phase of the prepared catalysts were analyzed by X-ray diffraction (XRD, Bruker of D8 Advance) using Cu Kα source, 2θ in range of 20º to 80º.

4.3.2 X-ray photoelectron spectroscopy

To determine the type of metal carbide, nitride and oxides species on the surface layer of catalysts were performed using the Kratos Amicus x-ray photoelectron spectroscopy (XPS) spectra, which worked at a power of 240 W with the x-ray source at 20 mA. The survey spectra were recorded using a pass energy of 75 eV and a step size of 0.1 eV/step under pressure about 1×10^{-6} Pa.

4.3.3 N_2 Sorption

The specific surface area, pore-volume, and pore size diameter of catalyst were determined from the N_2 adsorption-desorption isotherms by use a BEL SORP mini II device.

4.3.4 Scanning electron microscopy and Energy-dispersive x-ray spectroscopy (SEM and EDX)

Morphology and elemental distribution of prepared catalysts were analyzed by scanning electron microscopy and Energy-dispersive x-ray spectroscopy (SEM and EDX, Hitachi mode S-3400N for SEM while Link Isis series 300 program for EDX).

4.3.5 Thermogravimetric analysis

The carbon deposited on catalyst was measured by thermogravimetric analysis (TGA). The sample was heated up to 1000 ºC with the ramp rate of 10 ºC min^{-1} for measuring weight loss of spent catalysts.

4.4 Catalytic deoxygenation test

4.4.1 Pre-reduction process

After activation, the carbide and nitrite catalysts were removed from the quartz tube. The carbide and nitride catalysts were reduced under 100 ml min^{-1} of hydrogen flow at a heating rate of 5 ºC min^{-1} from room temperature to 450 ºC for 3 h. before the reaction test.

4.4.2 Activity test

The bio-hydrogenated diesel was carried out in a continuous flow trickle-bed reactor with a length of 50 cm and an inside diameter of 0.9 cm. The schematic diagram of the experimental equipment is shown in Figure 8. The catalyst with a volume of 6 ml was loaded into the reactor. All the catalysts were stabilized under operating conditions for 24 h. on stream. The operating conditions for the optimal operating conditions are shown in Table 7-10. The palm fatty acid distillate (PFAD) was preheated and feed to a continuous flow trickle-bed reactor controlled by a high-pressure pump and hydrogen flow rate was controlled by the mass flow controller.

จุฬาลงกรณ์มหาวิทยาลัย
Chulalongkorn University

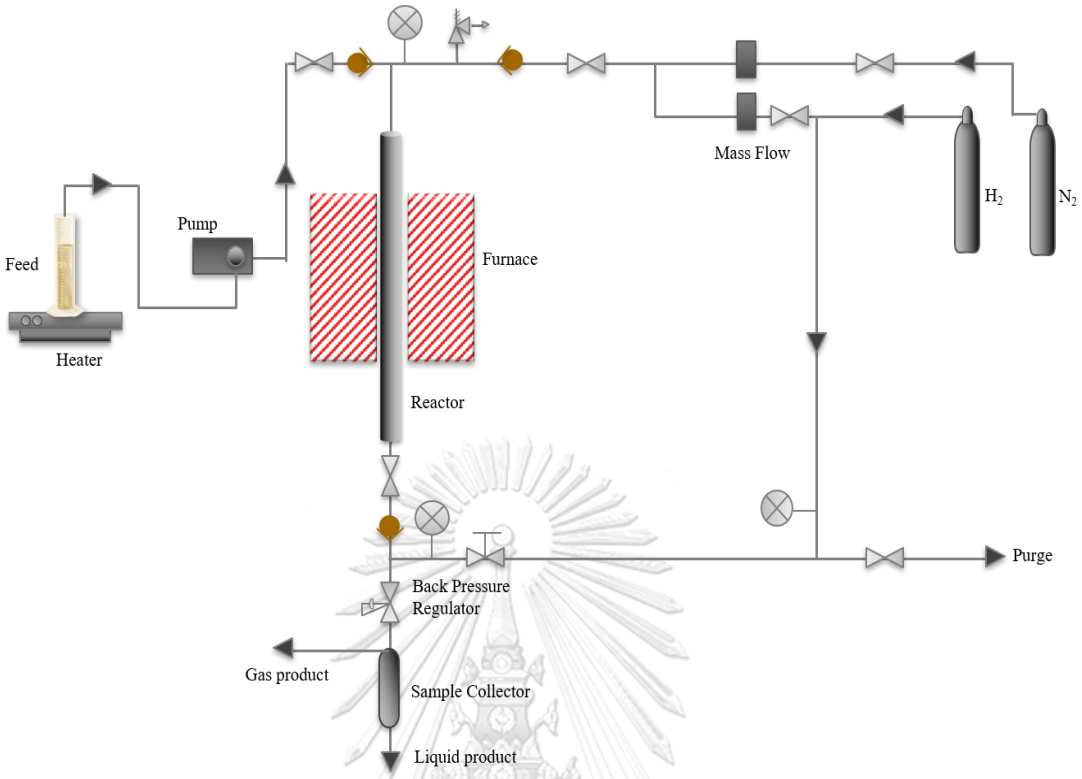

Figure 8 The schematic diagram of a continuous flow trickle bed reactor.

จุฬาลงกรณ์มหาวิทยาลัย
CHULALONGKORN UNIVERSITY

Table 9 Catalytic screening for green diesel via deoxygenation of palm fatty acid distillate.

Variable	Condition
Reactant	Palm fatty acid distillate (PFAD)
Temperature (ºC)	330
Hydrogen Pressure (MPa)	5
LHSV (h^{-1})	1
H_2 to oil ratio N($cm^3 \cdot cm^{-3}$)	1000
Catalyst type	MoN/Al, MoC/Al, CoMoC/Al, CoMoN/Al, NiMoC/Al and NiMoN/Al
Catalyst preparation method	Single-step decomposition

Table 10 Comparison of bimetallic transition carbide catalyst for green diesel via deoxygenation of palm fatty acid distillate.

Variable	Condition
Reactant	Palm fatty acid distillate (PFAD)
Temperature (ºC)	330
Hydrogen Pressure (MPa)	5
LHSV (h^{-1})	1
H_2 to oil ratio N($cm^3 \cdot cm^{-3}$)	1000
Catalyst type	CoMoC/Al, NiMoC/Al, CoMoC/Al-TPR and NiMoC/Al-TPR
Catalyst preparation method	Single-step decomposition and Temperature program reduction

จุฬาลงกรณ์มหาวิทยาลัย
Chulalongkorn University

Table 11 Optimization of the reaction parameter for green diesel via deoxygenation of palm fatty acid distillate.

Variable	Condition
Reactant	Palm fatty acid distillate
Temperature (ºC)	300, 330, 360 and 390
Hydrogen Pressure (MPa)	3 and 5
LHSV (h^{-1})	1
H_2 to oil ratio N($cm^3 \cdot cm^{-3}$)	1000
Catalyst type	CoMoC/Al and CoMoN/Al
Catalyst preparation method	Single-step decomposition

Table 12 Stability and deactivation study of the excellent catalysts for green diesel via deoxygenation of palm fatty acid distillate.

Variable	Condition
Reactant	Palm fatty acid distillate
Temperature (ºC)	330
Hydrogen Pressure (MPa)	5
LHSV (h^{-1})	1
H_2 to oil ratio N($cm^3 \cdot cm^{-3}$)	1000
Catalyst type	CoMoC/Al and CoMoN/Al
Catalyst preparation method	Single-step decomposition

จุฬาลงกรณ์มหาวิทยาลัย
Chulalongkorn University

4.4.3 FT-IR

The functional group of palm fatty acid distillate (PFAD) and liquid products were measured by the Fourier transform infrared (FTIR) spectroscopy (Perkin Elmer spectrum GXFT-IR).

4.4.4 Analysis of liquid and gas products

The liquid product and gaseous product were collected every 3 intervals. The gas product was analyzed by gas chromatography (GC, Shimadzu model GC-14B) equipped with thermal conductivity detector (TCD). The liquid product was analyzed gas chromatography equipped with flame ionization detector (FID). The operating conditions for the instruments are shown in Table 11-12. The conversion, gasoline selectivity, diesel selectivity, gasoline yield and diesel yield of the products were determined by the following Equations (1)–(4) and (5), respectively.

$$\text{Conversion}(-) = \frac{\text{Feed}_{FA+TG} - \text{Product}_{FA+TG}}{\text{Feed}_{FA+TG}} \quad (1)$$

$$\text{Gasoline selectivity}(-) = \frac{\text{Product}_{C_5-C_{11}} - \text{Feed}_{C_5-C_{11}}}{\text{Feed}_{FA+TG} - \text{Product}_{FA+TG}} \quad (2)$$

$$\text{Diesel selectivity}(-) = \frac{\text{Product}_{C_{12}-C_{18}} - \text{Feed}_{C_{12}-C_{18}}}{\text{Feed}_{FA+TG} - \text{Product}_{FA+TG}} \quad (3)$$

จุฬาลงกรณ์มหาวิทยาลัย
CHULALONGKORN UNIVERSITY

$$\text{Gasoline yield} = \text{liquid fraction} \times \text{conversion} \times \text{gasoline selectivity} \quad (4)$$

$$\text{Diesel yield} = \text{liquid fraction} \times \text{conversion} \times \text{diesel selectivity} \quad (5)$$

Where

$Feed_{FA+TG}$ is the weight percent of fatty acid and triglyceride in Feed.

$Product_{FA+TG}$ is the weight percent of fatty acid and triglyceride in product

$Fee_{C_5–C_{11}}$ and $Product_{C_5–C_{11}}$ are the percent of alkanes at a boiling point in the range of C_5–C_{11} in feed and product, respectively.

$Feed_{C_{12}–C_{18}}$ and $Product_{C_{12}–C_{18}}$ are the percent of alkanes at a boiling point in the range of C_{12}–C_{18} in feed and product, respectively. Gas and liquid fraction can be calculated from equations (6) and (7), respectively.

$$\text{Liquid fraction} = \frac{\text{weight of liquid product}}{\text{weight of feed}} \quad (6)$$

$$\text{Gas fraction} = 1 - \frac{\text{weight of liquid product}}{\text{weight of feed}} \quad (7)$$

Where

Gasoline yield = liquid fraction x conversion x gasoline selectivity
Diesel yield = liquid fraction x conversion x diesel selectivity
Yield of liquid fuel = diesel yield + gasoline yield

จุฬาลงกรณ์มหาวิทยาลัย
Chulalongkorn University

4.4.5 The maximum theoretical yields

The maximum theoretical yields of deoxygenated products were calculated based on the compositions of 6.8 wt.% of triglyceride and 93.2 wt.% of fatty acid contained in PFAD (See Table 1). The maximum theoretical yields of HDO and DCO_x ($DCO+DCO_2$) reaction pathway were determined by the following Equations (8) and (9), respectively.

The maximum theoretical yields of HDO = HDO (FFA) + HDO (TG) (8)

The maximum theoretical yields of DCO_x = DCO_x (FFA) + DCO_x (TG) (9)

Where

$$\text{HDO (FFA)} = \frac{Mw_{C_nH_{2n+2}}}{Mw_{\text{fatty acid}}} \times \%\ \text{FFA distribution in PFAD} \times 93.2\ \%\ \text{of FFA}$$

$$\text{HDO (TG)} = \frac{Mw_{C_nH_{2n+2}}}{Mw_{\text{triglyceride}}} \times \%\ \text{FFA distribution in PFAD} \times 6.8\ \%\ \text{of TG}$$

$$DCO_x\ \text{(FFA)} = \frac{Mw_{C_nH_{2n+2}}}{Mw_{\text{fatty acid}}} \times \%\ \text{FFA distribution in PFAD} \times 93.2\ \%\ \text{of FFA}$$

$$DCO_x\ \text{(TG)} = \frac{Mw_{C_nH_{2n+2}}}{Mw_{\text{triglyceride}}} \times \%\ \text{FFA distribution in PFAD} \times 6.8\ \%\ \text{of TG}$$

จุฬาลงกรณ์มหาวิทยาลัย
Chulalongkorn University

Table 13 Operating condition in Gas Chromatography – Flame Ionization Detector (GC-FID).

Gas chromatograph	Condition
Detector	FID
Column	DB-1HT
Carrier gas	He
Split	30 ml min^{-1}
Purge	4 ml min^{-1}
Make up pressure	40 kPa
Carrier pressure	40 kPa
Detector temperature	370 °C
Column temperature	40 °C ramp 8 °C min^{-1} to held at 270 °C for 11 min, and increase of 15 °C min^{-1} to 370 °C and held for 15 min
Injector temperature	340 °C

จุฬาลงกรณ์มหาวิทยาลัย
Chulalongkorn University

Table 14 Operating condition in Gas Chromatography–Thermal Conductivity Detector (GC-TCD).

Gas chromatograph	Condition
Detector	TCD
Column	Porapak Q, MS5A
Carrier gas	Air (30 ml min^{-1})
Make up pressure	40 kPa
Carrier pressure	Ar 40 kPa
Detector temperature	150 °C
Column temperature	40 °C ramp 20 °C min^{-1} to held at 100°C for 11 min
Injector temperature	150 °C

จุฬาลงกรณ์มหาวิทยาลัย
Chulalongkorn University

CHAPTER V

RESULTS AND DISCUSSION

This chapter is divided into three main parts. In the first part, catalyst screening among carbide and nitride catalysts was investigated. The catalysts preparation was compared between a single-step decomposition method and the temperature-programmed reduction (TPR). In the second part, the effects of operating temperature and hydrogen pressure on the conversion, selectivity, yield, gas product composition and contribution of HDO and DCO_x were investigated.

5.1 Catalyst screening and comparison of bimetallic carbide catalysts

5.1.1 Catalyst characterization

5.1.1.1 X-ray diffraction (XRD)

The XRD patterns of the alumina-supported metal nitride catalysts are shown in Fig. 9. The diffraction peaks of cubic γ-Al_2O_3 at 37.5º, 46º and 67º were detected for all the catalysts [48-50]. The diffraction peaks of Mo_2N phase at 37.2º, 43.3º, 62.8º, and 75.4º for the Mo_2N supported on γ-Al_2O_3 catalyst could not be detected due to overlapping with peaks of γ-Al_2O_3 support [51, 52]. The diffraction peak at 32.50º, 35.54º 40.10º, 42.63º, 46.63º, 59.99º, 65.01º, 69.89º, 72.79º and 74.57º were attributed to the Co_3Mo_3N phase [51]. The peak at 30.22º, 40.92º, 43.32º, 45.46º, 51.65º, 59.18º, 72.81º and 77.74º were attributed to the Ni_3Mo_3N phase [51]. The XRD patterns of the alumina-supported metal carbide catalysts are shown in Figs. 9 and 10. In addition, the diffraction peaks at 34.7º, 38.0º, 39.8º, 52.26º, 62.1º, and 75.5º were assigned to Mo_2C phase observed in the Mo_2C supported on γ-Al_2O_3 catalyst [52]. The diffraction peaks at 39.9º, 42.6º and 46.5º attributed to the Co_3Mo_3C phase for the Co_3Mo_3C supported on γ-Al_2O_3 catalyst could not be detected due to overlapping with peaks of γ-Al_2O_3 support [44, 53]. The observed diffraction peaks at (d) graph were assigned to Ni_3Mo_3C phase (JCPDS no. 89-4883) [54].

CHULALONGKORN UNIVERSITY

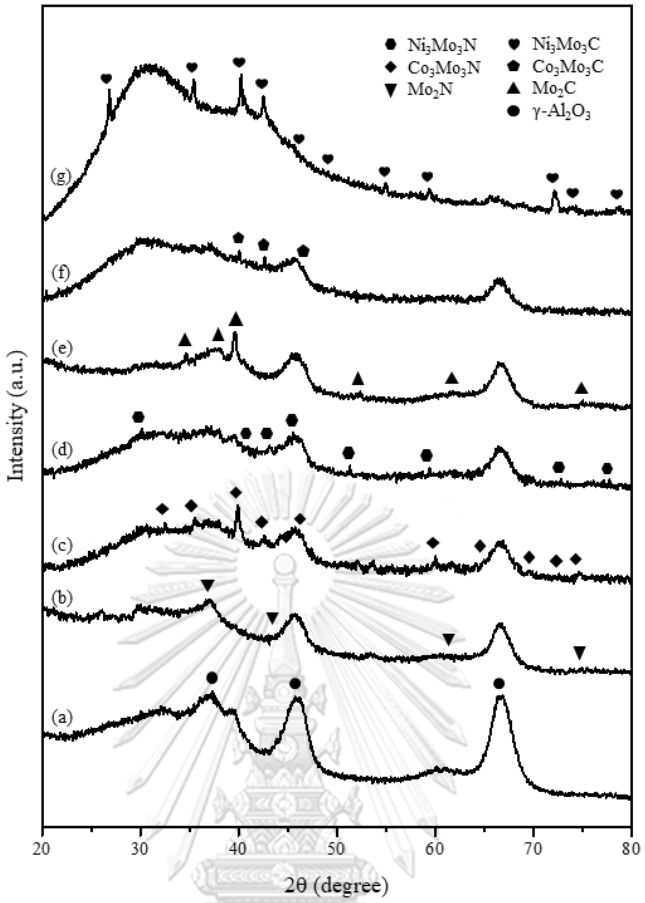

Figure 9 XRD patterns of the (a) γ-Al_2O_3 Support, (b) MoN/Al, (C) CoMoN/Al, (d) NiMoN/Al, (e) MoN/Al, (f) CoMoC/Al, and (g) NiMoN/Al catalysts.

จุฬาลงกรณ์มหาวิทยาลัย
Chulalongkorn University

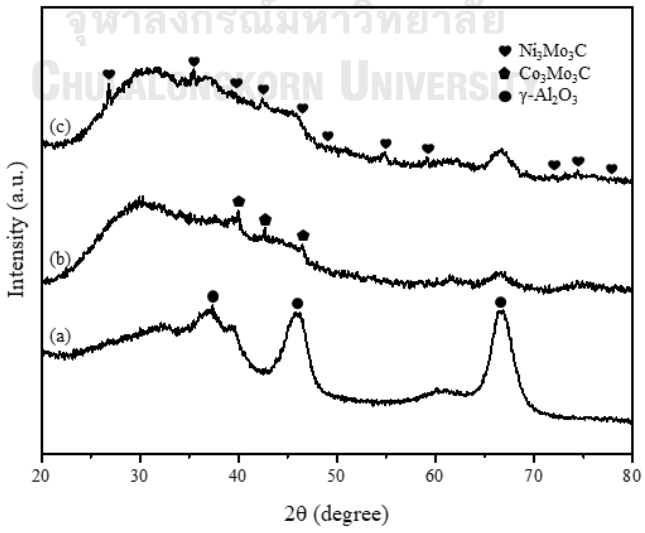

Figure 10 XRD patterns of the (a) γ-Al_2O_3 Support, (b) CoMoC/Al catalysts (TPR method), and (C) NiMoC/Al catalysts (TPR method).

5.1.1.1 X-ray photoelectron spectroscopy (XPS)

The XPS spectra of (a) MoC/Al, (b) CoMoC/Al, (c) NiMoC/Al, (d) CoMoC/Al-TPR, (e) NiMoC/Al-TPR, (f) MoN/Al, (g) NiMoN/Al and (h) CoMoN/Al catalysts are shown in Figure 11. The Mo $3d_{5/2}$ spectra at binding energy (BE) of 228.1, 228.4 and 228.5 eV are assigned to Mo^{2+} species [55-58]. While the Mo $3d_{3/2}$ spectra at binding energy (BE) of 231.9.eV are assigned to Mo^{2+} species [56]. Thus, the peak at 228.2±0.2 eV and 231.9 eV are ascribed to Mo^{2+} involved in Mo-C and M-N bonding of molybdenum carbide and nitride-based catalysts. The peak located at 232.0, 232.2, 232.5 and 232.9 eV were detected in Mo oxide phase corresponds to Mo $3d_{5/2}$ of Mo^{6+} species due to oxidation of catalyst surface [51, 56, 57, 59]. In addition, Mo $3d_{3/2}$ spectra at binding energy (BE) of 231.6, 235.2, 235.5 and 235.7 eV are assigned to Mo^{6+} species [56, 58, 59]. Thus, the peaks at 231.6, 232.4±5 and 235.2±4 represent Mo^{6+}species of molybdenum carbide and nitride-based catalysts.

จุฬาลงกรณ์มหาวิทยาลัย
Chulalongkorn University

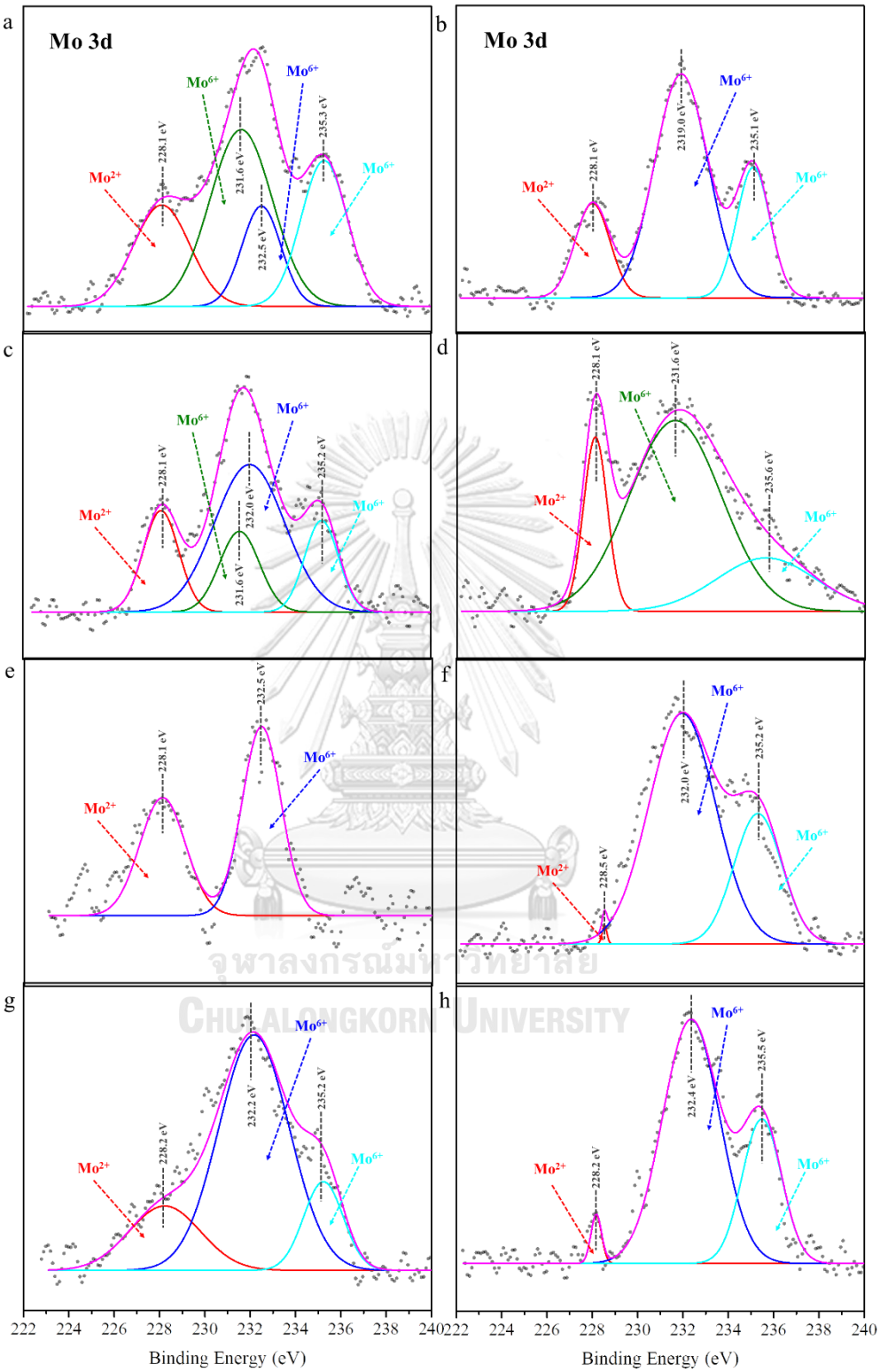

Figure 11 Mo3d spectra of (a) MoC/Al, (b) CoMoC/Al, (c) NiMoC/Al, (d) CoMoC/Al-TPR, (e) NiMoC/Al-TPR, (f) MoN/Al, (g) CoMoN/Al and (h) NiMoN/Al catalysts.

5.1.1.2 N_2 Physisorption

Table 15 Physical properties of the fresh catalysts.

Catalysts	Surface area ($m^2 \cdot g^{-1}$)	Total pore volume ($cm^3 \cdot g^{-1}$)	Mean pore diameter (nm)
γ-Al_2O_3	232	0.73	12.58
MoC/Al	123	0.35	11.22
MoN/Al	121	0.35	11.75
CoMoC/Al	193	0.58	11.95
CoMoN/Al	186	0.50	10.82
NiMoC/Al	179	0.54	12.05
NiMoN/Al	171	0.47	11.04
CoMoC/Al-TPR	190	0.55	11.43
NiMoC/Al-TPR	172	0.49	11.74

จุฬาลงกรณ์มหาวิทยาลัย
Chulalongkorn University

Table 13 summarizes the BET specific surface areas, total pore and means pore diameter of MoC/Al, MoN/Al, CoMoC/Al, CoMoN/Al, NiMoC/Al, NiMoN/Al CoMoC/Al-TPR and NiMoC/Al-TPR catalysts. The BET specific surface areas and total pure volume increased in the order of CoMoC/Al > CoMoC/Al-TPR > CoMoN/Al > NiMoC/Al > NiMoC/Al-TPR > NiMoN/Al > MoC/Al > MoN/Al catalysts.

The BET specific surface area and total pore volume of the γ-Al_2O_3 support decreased with metal loading of Mo, Co and Ni species. As a result of the pore structure of pure γ-Al_2O_3 support was filled or blocked by metals (Mo, Co and Ni) species. In contrast, average pore diameter of all the catalyst did not significantly change after impregnation of metal species.

N_2 adsorption/desorption isotherm of fresh catalysts are shown in Figure 12. The N_2 adsorption/desorption isotherm of all the catalysts show type IV adsorption isotherms, indicating the mesoporous structure of all γ-Al_2O_3 supported catalysts. Moreover, the area of the hysteresis loop of MoC/Al and MoN/Al catalysts was decreased, indicating that the pores of catalysts were blocked by Mo species [60, 61]. These were consistent with the BET specific surface area and total pore volume of both catalysts (See Table 13).

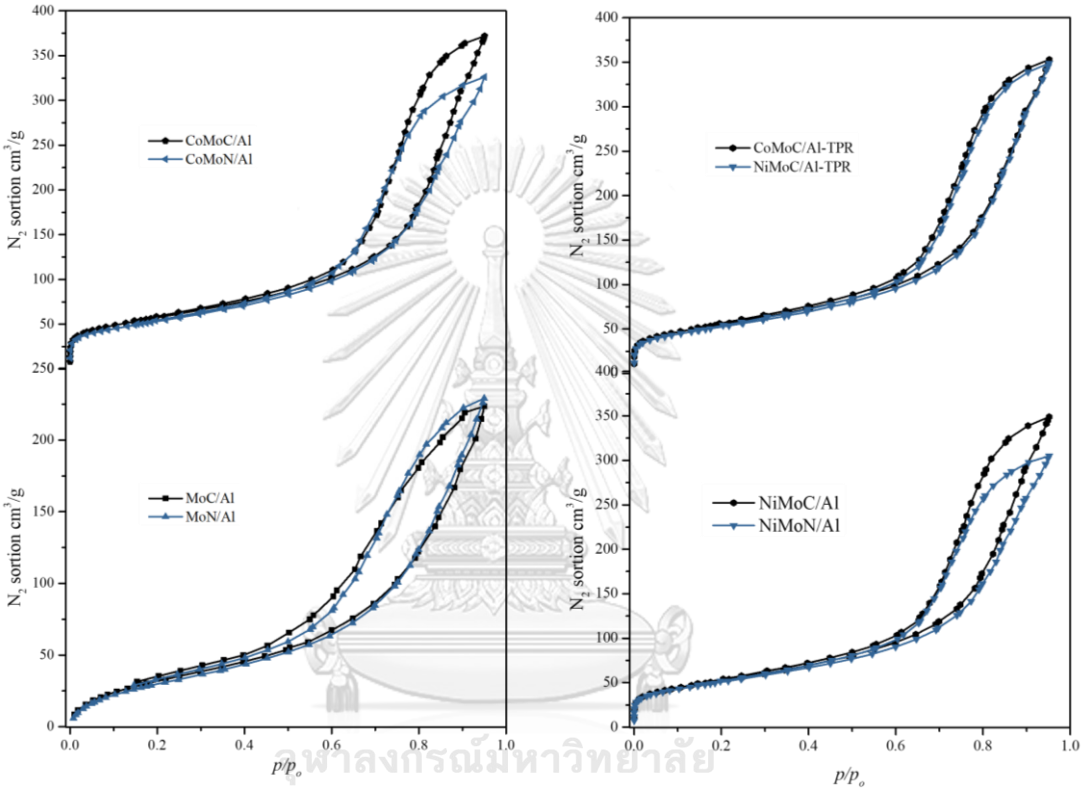

จุฬาลงกรณ์มหาวิทยาลัย
CHULALONGKORN UNIVERSITY

Figure 12 N_2 adsorption/desorption isotherm of MoC/Al, MoN/Al, CoMoC/Al, CoMoN/Al, NiMoC/Al and NiMoN/Al catalysts.

5.1.1.3 Scanning electron microscopy and Energy-dispersive x-ray spectroscopy (SEM and EDX)

Table 16 Elemental distribution of the fresh catalysts.

Catalysts	Elements (wt.%)							
	Mo	**Al**	**O**	**Co**	**Ni**	**C**	**N**	**Mo/Metal**
MoC/Al	19.9	47.4	28.9	-	-	3.3	0.6	-
MoN/Al	19.5	45.8	30.6	-	-	2.9	1.2	-
CoMoC/Al	12.9	47.5	28.4	7.3	-	3.1	0.9	1.1
CoMoN/Al	12.7	45.5	28.8	7.2	-	4.0	1.9	1.1
NiMoC/Al	12.3	46.7	29.4	-	7.4	3.8	0.7	1.0
NiMoN/Al	12.3	45.5	28.7	-	7.6	3.8	1.2	1.0
CoMoC/Al-TPR	13.1	45.9	27.9	8.5	-	4.6	0.0	0.9
NiMoC/Al-TPR	12.7	46.1	29.1	-	7.4	4.8	0.0	1.1

The fresh catalysts were characterized by energy-dispersive x-ray spectroscopy (EDX) to examine metal content in catalysts. The elemental contents of the fresh catalysts are summarized in Table 14. It was found that metal content in catalysts was 20% according to percent loading in catalyst preparation. The mole of Mo to Co or Ni was 1:1, which corresponded to the equivalent mole of the metal in the catalyst preparation.

The SEM images of (a) MoC/Al, (b) MoN/Al, (c) CoMoC/Al, (d) CoMoN/Al, (e) NiMoC/Al, (f) NiMoN/Al, (g) CoMoC/Al-TPR and (h) NiMoC/Al-TPR catalysts are shown in Figure 13. The SEM images of MoC/Al and MoN/Al catalysts (Figure 12a and b) exhibited an agglomerated angular particles [51]. The addition of Co and Ni slightly changed the structures of the catalysts. The SEM images of CoMoC/Al, CoMoN/Al, NiMoC/Al, NiMoN/Al, CoMoC/Al-TPR, and NiMoC/Al-TPR catalysts (Figure 12c-h) indicated irregular particles with a size of 0.1-0.2 μm [62, 63].

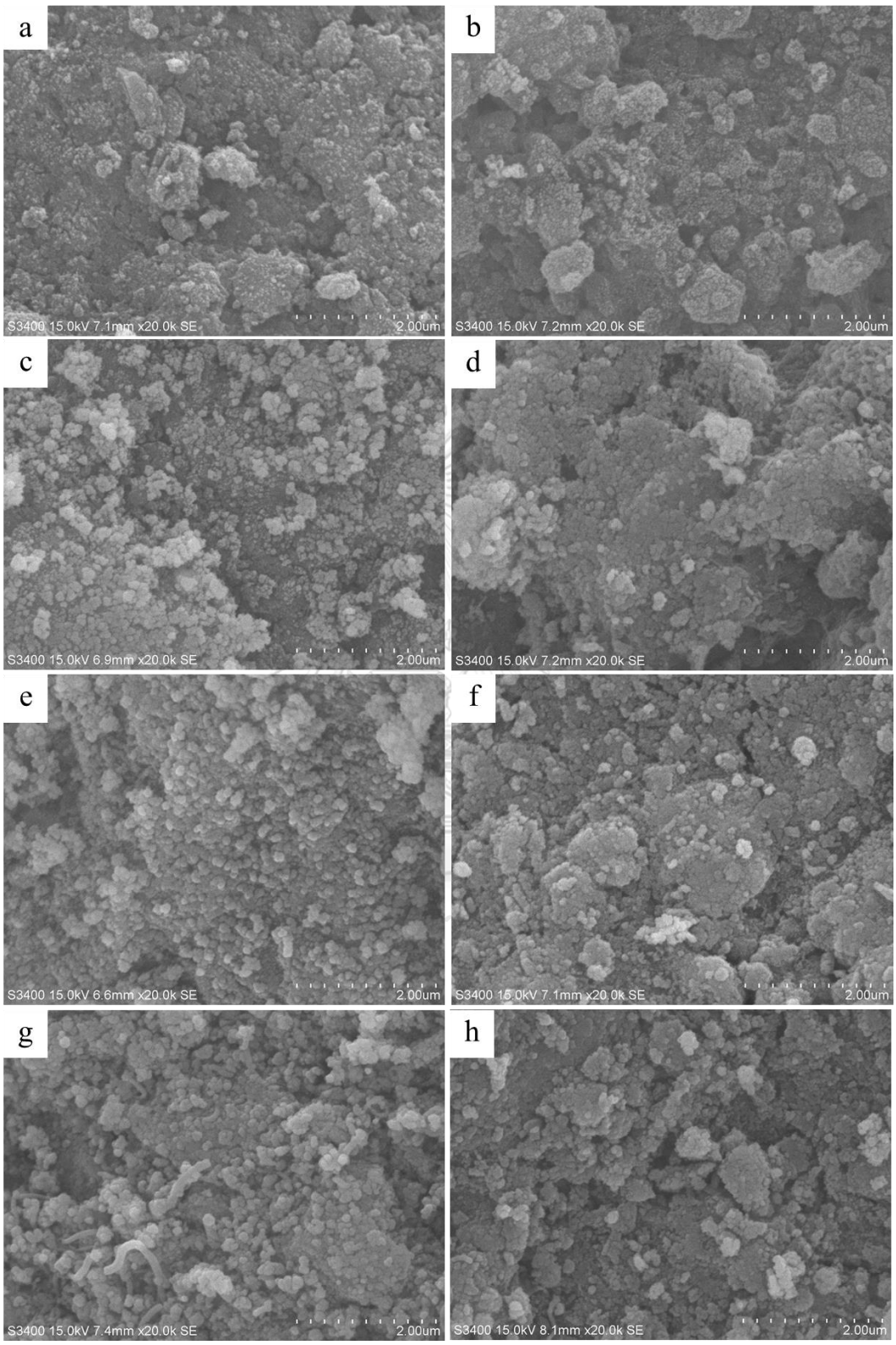

Figure 13 SEM images of (a) MoC/Al, (b) MoN/Al, (c) CoMoC/Al, (d) CoMoN/Al, (e) NiMoC/Al, (f) NiMoN/Al, (g) CoMoC/Al-TPR and (h) NiMoC/Al-TPR catalysts.

5.1.1.4 Thermogravimetric analysis (TGA)

The TGA profiles of spent catalysts after the hydrotreating of PFAD are exhibited in Figure 14. The weight loss with increasing temperature consists of three-stages at a temperature of 50 ˚C to 250 ˚C, 250 ˚C to 350 ˚C, and 350 ˚C to 600 ˚C, which corresponded to the loss of moisture, physical absorbents, and formation of coke (soft and hard), respectively [64]. The total weight loss was 12.8%, 14.2%, 14.7%, 15.3%, 15.7%, 17.1%, 17.3% and 20.2% for the CoMoC/Al, CoMoC/Al-TPR, MoC/Al, NiMoC/Al, MoN/Al, CoMoN/Al, NiMoC/Al-TPR, and NiMoN/Al catalysts, respectively. The amount of carbon deposition of nitride catalysts was higher than that of carbide catalysts of the deactivation of nitride catalysts during the deoxygenation reaction.

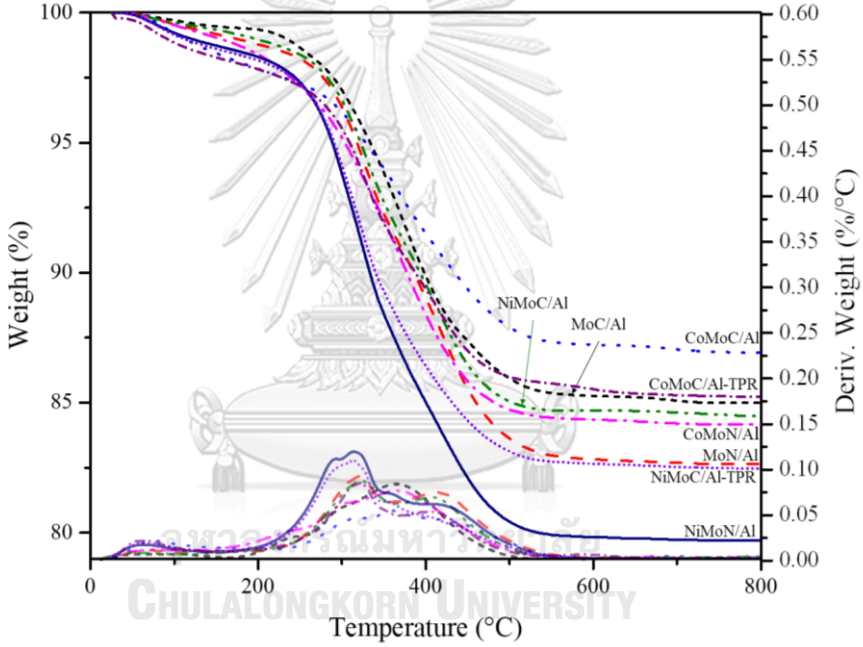

Figure 14 TG/DTG profiles of the spent catalysts. The operating condition at a temperature of 330 °C, 5 MPa of hydrogen pressure, 1 h^{-1} of LHSV and 1000 N($cm^3 \cdot cm^{-3}$) of H_2/feed ratio.

5.1.2 Catalysis screening

This section studied the effect of metal loading for the Mo carbide and nitride catalysts. Excellent catalysts in carbide and nitride phases were selected for further optimization on the operation conditions and catalytic stability test.

Table 17 Catalytic actives for deoxygenation of palm fatty acid distillate over carbide and nitride catalysts.

Catalysts	Conversion (%)	Selectivity (%)		Yield (%)		Product phase	Product color
		Diesel selectivity	Gasoline selectivity	Diesel yield	Gasoline yield		
MoC/Al	71	99.5	0.5	56.4	0.3	Solid+ Liquid	Light brown
MoN/Al	40	99.3	0.7	32.2	0.2	Solid	Light brown
CoMoC/Al	98	99.3	0.7	84.8	0.6	Liquid	Clear
CoMoN/Al	94	98.8	1.2	67.1	0.8	Liquid	Yellow
NiMoC/Al	98	99.6	0.4	78.1	0.3	Liquid	Clear
NiMoN/Al	73	99.4	0.6	61.8	0.4	Solid+ Liquid	Light brown

จุฬาลงกรณ์มหาวิทยาลัย
Chulalongkorn University

The catalytic actives for deoxygenation of palm fatty acid distillate over carbide and nitride catalysts. are summarized in Table 15 and the conversion and diesel yield are shown in Figure 15a. All supported catalysts (MoC/Al, MoN/Al, CoMoC/Al, CoMoN/Al, NiMoC/Al and NiMoN/Al) were investigated to examine the activity of the catalyst on deoxygenation reaction under a temperature of 330 °C, 5 MPa of hydrogen pressure, 1 h^{-1} of LHSV and 1000 N($cm^3 \cdot cm^{-3}$) of H_2/feed ratio.

In case of the monometallic catalysts, MoC/Al catalyst exhibited the highest conversion in compared with the MoN/Al catalyst. This result was in agreement with those of Akhmetzyanova et al. [65] and Carmona et al. [66]. A comparison between monometallic and bimetallic carbide and nitride catalysts showed the difference in activity. Bimetallic carbide catalysts showed the highest conversion and diesel yield of 73% to 98% and 61.8% to 84.8%, respectively. In contrast, conversion and diesel yield of monometallic carbide and nitride catalysts were in the ranges of 40% to 71%

and 32.2% to 56.4%, respectively. These results were consistent with those of preceding studies [67, 68]. CoMoC/Al catalyst showed the highest conversion and diesel yield of 98% and 84.8%, respectively. CoMoN/Al catalyst showed the highest conversion and diesel yield in the nitride phase of 94% and 67.1%, respectively. Product phase of MoC/Al, MoN/Al, and NiMoN/Al catalyst showed solid phase as a result of low PFAD conversion. Moreover, product color corresponded to the activity of catalysts. Hight conversion and diesel yield of the product are a clear color similar to diesel petroleum fuel.

The maximum theoretical yields of deoxygenated products were calculated based on the compositions of 93.2 wt.% of fatty acid and 6.8 wt.% of triglyceride contained in PFAD are shown in figure 15a. The maximum theoretical yields were 83.7% and 88.9% of DCO_x and HDO reaction pathways, respectively.

The Effect of catalysts on contribution of HDO and DOC_x are shown in Figure 15c. All catalysts promote the hydrodeoxygenation (HDO) pathway, which consisted of high normal alkane of $C_{14}H_{30}$, $C_{16}H_{34}$ and $C_{18}H_{38}$. The contribution of HDO decreased in order of CoMoC/Al > MoC/Al > NiMoC/Al > CoMoN/Al > NiMoC/Al > MoN/Al. HDO pathway could remove oxygen of free fatty acid in the form of water as a by-product. As a result, the number of carbon atom is same as the number of carbon atom in feedstock (oleic acid and palmitic acid mostly). On the other hand, decarboxylation (DCO_2) and decarbonylation (DCO) pathway consisted of normal alkane of $C_{15}H_{32}$ and $C_{17}H_{36}$. Contribution of DCO_x decrease in order of MoN/Al > NiMoC/Al > CoMoN/Al > NiMoN/Al > MoC/Al > CoMoC/Al. While DCO_x consists of DCO and DCO_2. The DCO pathway could remove oxygen of free fatty acid and the carbon atom content in the feedstock in the form of CO. The DCO_2 pathway could remove oxygen of free fatty acid and the carbon atom content in the feedstock in the form of CO_2. Therefore, the DCO pathway is the main pathway in $\%DCO_x$ contribution because CO is mainly gas product compositions as shown in Figure 15b.

Gas product compositions are shown in Figure 15b. CO and CO_2 gas are by-product of DCO_x pathway of deoxygenation reaction. While CH_4 generated by methanation of H_2 and CO_2 (Figure 5). Moreover, CO reacts with H_2O to generate CO_2 by a water gas shift (Figure 5). Gas product compositions decreased in order to CoMoN/Al > NiMoC/Al > CoMoC/Al > NiMoN/Al > MoC/Al > MoN/Al, which relate to $\%DCO_x$ contribution and PFAD conversion.

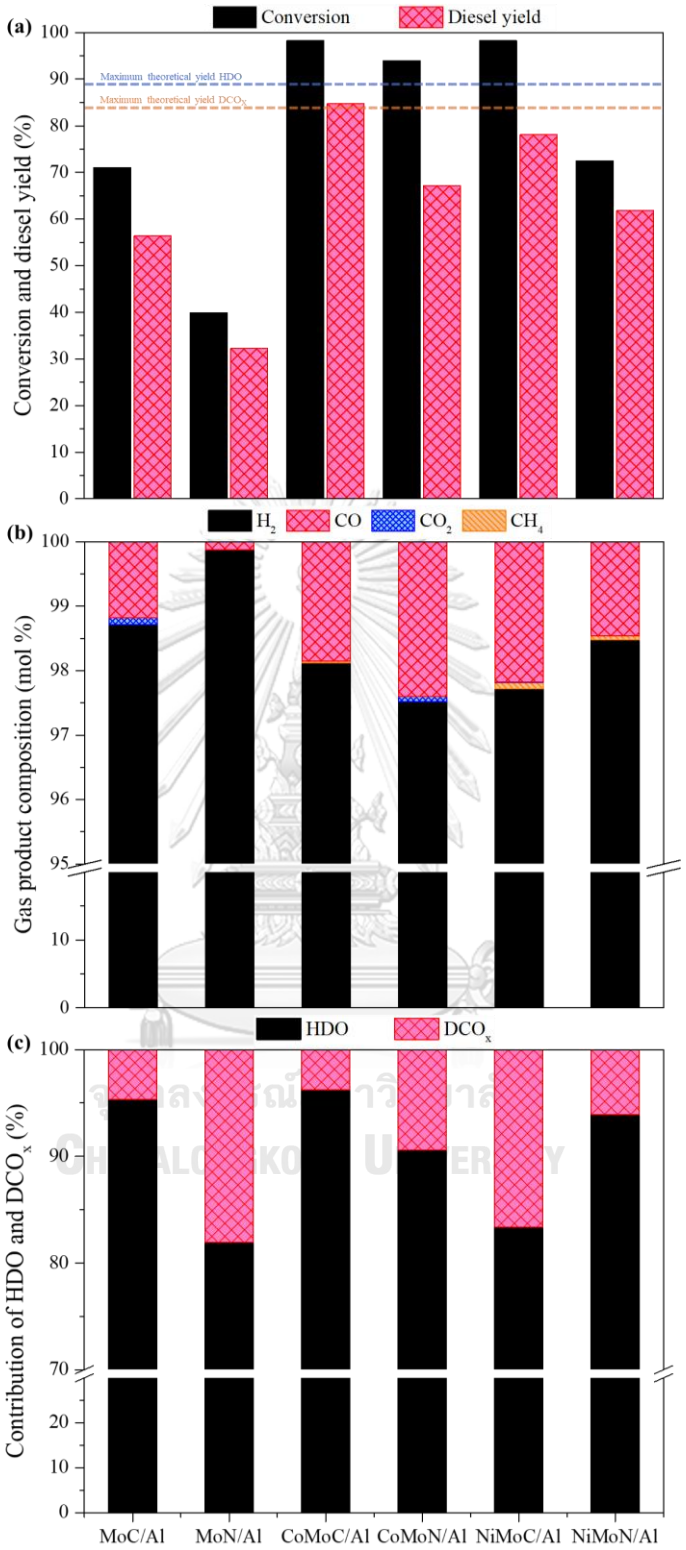

Figure 15 Effect of catalysts on (a) conversion and diesel yield (b) gas product composition (c) liquid product composition and contribution of HDO and DCO_x were performed at a temperature of 330 °C, 5 MPa of hydrogen pressure, 1 h^{-1} of LHSV and 1000 N($cm^3 \cdot cm^{-3}$) of H_2/feed ratio.

The functional group of the liquid products and feed characterized by Fourier transform infrared (FTIR) spectroscopy are shown in Figure 16. The triglyceride is represented by peaks at 1746 cm^{-1} and 1164 cm^{-1} which are corresponding to carbonyl group (-C=O stretch) and acid or ester groups (-C-O stretch), respectively [13]. Peak at 1704 cm^{-1} corresponded to the carboxylic acid functional group of fatty acid detected in fatty acid [13, 69]. The aliphatic hydrocarbons generated from stretching, bending and rocking vibration of aliphatic hydrocarbons showed at 3000–2800, 1465–1377 and 720 cm^{-1}, respectively. Peaks at 3008 and 970 cm^{-1}, corresponded to C–H stretching and C–H out of plane bending, respectively [69]. Fatty acid and triglyceride peaks are represented in palm fatty acid distillate feedstock, which the fatty acid peak shows higher peak intensity than triglyceride peaks, represents high fatty acid content in PFAD. Fatty acid and triglyceride peaks were present in palm fatty acid distillate feedstock and they were absent in green diesel fuel spectrums. Because triglyceride and fatty acid were converted to green diesel fuel. Fatty acid and triglyceride peaks were not observed in CoMoC/Al and NiMoC/Al catalysts as they were completely converted to green diesel fuel. In contrast, Fatty acid and triglyceride peaks in the product present the incomplete conversion to green diesel fuel via the MoC/Al, MoN/Al, CoMoN/Al and NiMoN/Al catalysts. The FTIR results corresponded well with a conversion resuits of all catalysts (See Table 15).

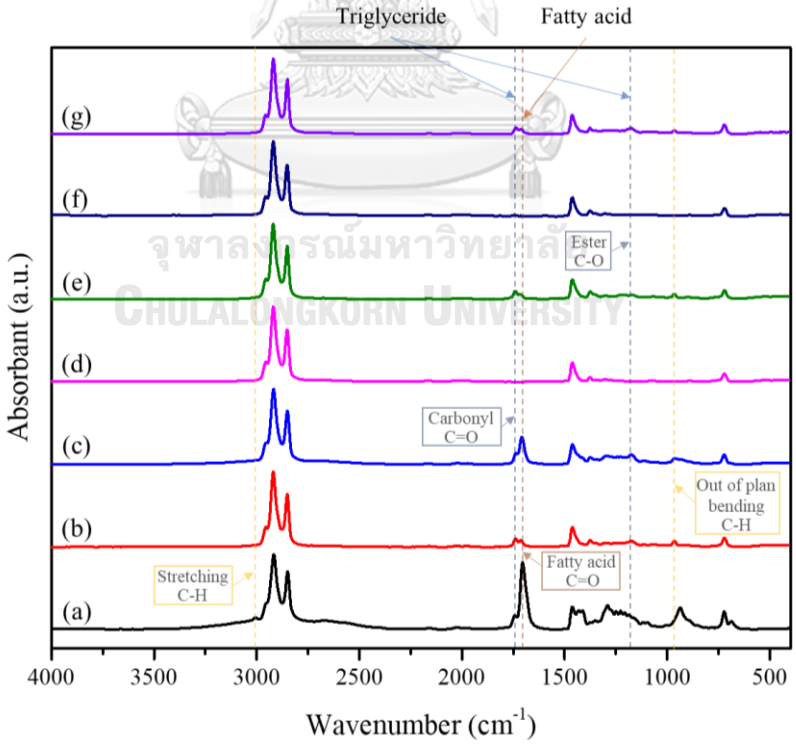

Figure 16 The FT-IR spectra of liquid products catalyzed by (a) PFAD, (b) MoC/Al, (c) MoN/Al, (d) CoMoC/Al, (e) CoMoN/Al, (f) NiMoC/Al and (g) NiMoN/Al catalysts.

5.1.3 Comparison of bimetallic carbide catalyst

In this section, the preparation of bimetallic carbide catalysts (CoMoC/Al and NiMoC/Al) was comparisons between the temperature-programmed reduction method (TPR) and the single-step decomposition method. The effect of the preparation method studied on conversion, selectivity, yield and reaction pathway (contribution of HDO and DCO_x) were performed at a 330 ˚C of temperature, 5 MPa of hydrogen pressure, 1 h^{-1} LHSV and 1000 N($cm^3 \cdot cm^{-3}$) of H_2/feed ratio.

Table 18 Effect of preparation method for bimetallic carbide catalysts on conversion, selectivity, yield, product phase and product color.

Catalysts	Conversion (%)	Selectivity (%)		Yield (%)		Product phase	Product color
		Diesel selectivity	Gasoline selectivity	Diesel yield	Gasoline yield		
CoMoC/Al	98	99.3	0.7	84.8	0.6	Liquid	Clear
CoMoC/Al -TPR	99	99.3	0.7	79.6	0.6	Liquid	Clear
NiMoC/Al	98	99.6	0.4	78.1	0.3	Liquid	Clear
NiMoC/Al-TPR	98	99.4	0.6	74.1	0.4	Liquid	Yellow

จุฬาลงกรณ์มหาวิทยาลัย
Chulalongkorn University

The effect of preparation method for bimetallic carbide catalysts on conversion, selectivity, yield, product phase and product color are summarized in Table 16. PFAD conversion and diesel yield are shown in Figure 17a. The deoxygenation of palm fatty acid distillate over CoMoC/Al and NiMoC/Al catalysts prepared by the single-step decomposition method and CoMoC/Al-TPR and NiMoC/Al-TPR prepared by catalysts by the temperature-programmed reduction method (TPR) were performed at a temperature of 330 °C, 5 MPa of hydrogen pressure, 1 h^{-1} of LHSV and 1000 N($cm^3 \cdot cm^{-3}$) of H_2/feed ratio.

The diesel yield of bimetallic carbide catalysts decreased in order to CoMoC/Al > CoMoC/Al-TPR > NiMoC/Al > NiMoC/Al-TPR. The bimetallic carbide catalysts prepared by the single-step decomposition method were slightly higher activity than the catalysts prepared by temperature-programmed reduction method (TPR). The single-step decomposition method (See Table 13) lead to higher larger pore volumes and surface areas, which improves the activity of the catalysts. That accorded the previous report on the comparison between the temperature-programmed reduction method and the single-step decomposition methods [62]. In addition, the single-step decomposition method is a simple method for the preparation of CoMoC/Al and NiMoC/Al catalysts.

The gas product composition of bimetallic carbide catalysts is shown in Figure 17b. The gas product composed of 1.8 mol%-2.3 mol% of mixed CO, CO_2 and CH_4 for all bimetallic carbide catalysts, which corresponds to a high contribution of HDO pathway in Figure 17c. Because HDO doesn't generate gas, as a by-product.

จุฬาลงกรณ์มหาวิทยาลัย
Chulalongkorn University

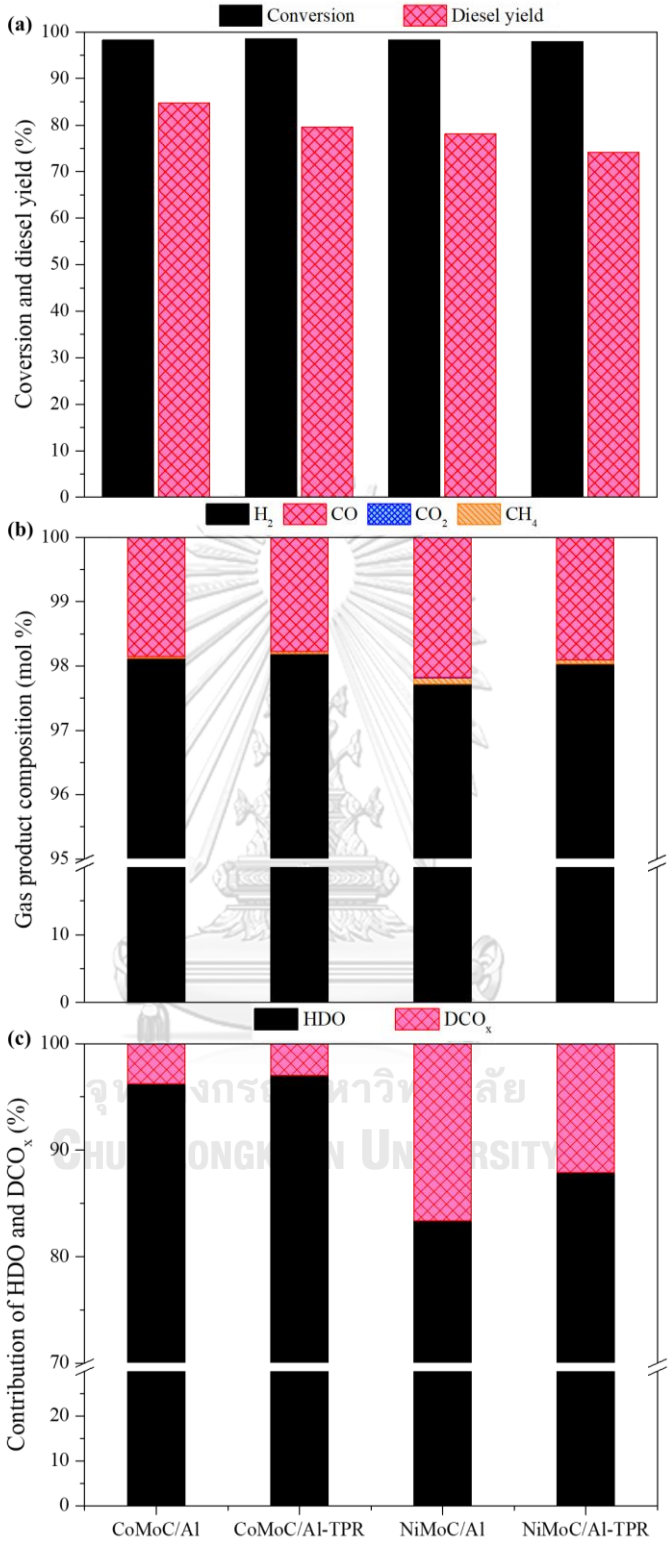

Figure 17 Effect of preparation method for bimetallic carbide catalysts on (a) conversion and diesel yield, (b) gas product composition, (c) contribution of HDO and DCO_x were performed at a temperature of 330 °C, 5 MPa of hydrogen pressure, 1 h^{-1} of LHSV and 1000 N($cm^3 \cdot cm^{-3}$) of H_2/feed ratio.

The functional group of liquid products catalyzed by CoMoC/Al, CoMoC/Al-TPR, NiMoC/Al, NiMoN/Al-TPR catalysts and PFAD feedstock were characterized by Fourier transform infrared (FTIR) spectroscopy are shown in Figure 18. Triglyceride and free fatty acids peak cannot be observed in green diesel spectrums of bimetallic carbide catalysts, confirming that he bimetallic carbide catalysts prepared by the single-step decomposition and TPR methods completely converted to green diesel products.

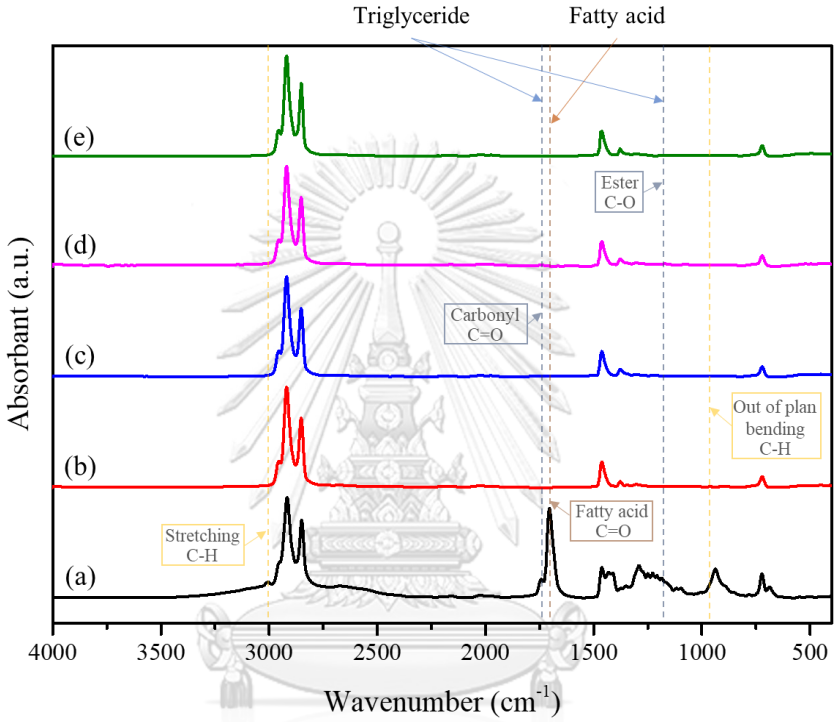

จุฬาลงกรณ์มหาวิทยาลัย
Chulalongkorn University

Figure 18 The FT-IR spectrums of liquid products catalyzed by (a) PFAD, (b) CoMoC/Al, (c) CoMoC/Al-TPR, (d) NiMoC/Al and (e) NiMoN/Al-TPR catalysts.

5.2 Optimal operating parameter

In this section, the effect of operating temperature and hydrogen pressure on the conversion, selectivity, yield, gas product composition and contribution of HDO and DCO_x were investigated. The temperature was investigated in the range of 300 ˚C to 390 ˚C and hydrogen pressure was studied at 3 MPa and 5 MPa with fixed the other conditions: 1 h^{-1} of LSHV and 1000 N($cm^3 \cdot cm^{-3}$) of H_2/Feed ratio. The CoMoC/Al and CoMoN/Al catalysts were selected to study effect of temperature and pressure on the activity of the catalysts.

จุฬาลงกรณ์มหาวิทยาลัย
Chulalongkorn University

Table 19 Effects of temperature and hydrogen pressure on conversion, selectivity, yield, product phase and product color.

Catalysts	Parameter	T. (˚C)	P. (MPa)	Conversion (%)	Selectivity (%)		Yield (%)		Product phase	Product color
					Diesel selectivity (%)	Gasoline selectivity (%)	Diesel yield (%)	Gasoline yield (%)		
CoMoC/Al	Temp.	300	5	84	99.5	0.5	75.6	0.4	Liquid	Yellow
		330	5	98	99.3	0.7	84.8	0.6	Liquid	Clear
		360	5	99	98.2	1.8	75.7	1.3	Liquid	Light green
		390	5	99	97.2	2.8	73.7	2.1	Liquid	Light green
	Pressure	330	3	96	99.3	0.7	82.9	0.6	Liquid	Clear
		330	5	98	99.3	0.7	84.8	0.6	Liquid	Clear
CoMoN/Al	Temp.	300	5	54	97.8	2.2	39.4	0.9	Solid+ Liquid	Light brown
		330	5	94	98.8	1.2	67.1	0.8	Liquid	Yellow
		360	5	97	98.3	1.7	69.6	1.2	Liquid	Clear
		390	5	96	97.2	2.8	69.8	2.0	Liquid	Light green
	Pressure	330	3	91	98.8	1.2	64.7	0.8	Liquid	Yellow
		330	5	94	98.8	1.2	67.1	0.8	Liquid	Yellow

Chulalongkorn University

5.2.1 Effect of temperature

The effect of the temperature on the hydrotreating process was carried out using CoMoC/Al and CoMoN/Al catalysts in a continuous process. The temperature was studied in the range of 300 ˚C to 390 ˚C under fixed 5 MPa of hydrogen pressure, 1 h^{-1} of LSHV, and 1000 N($cm^3 \cdot cm^{-3}$) of H_2/feed ratio.

PFAD conversion and diesel yield of CoMoC/Al and CoMoN/Al catalysts are shown in Figure 19a. The optimal temperature of the deoxygenation reaction in a continuous process was 330 ˚C, which highest PFAD conversion and diesel yield of CoMoC/Al catalyst were 98% and 84.8%, respectively. While conversion and diesel yield of the temperature at 300 ˚C decreased to 84% and 75.6%, respectively because of the low activity of catalyst in low reaction temperature. At a temperature of 330 ˚C, PFAD conversion and diesel yield of CoMoN/Al catalyst were 94% and 67.1%, respectively. While the conversion and diesel yield of CoMoN/Al catalyst from temperature of 300 ˚C were 54% and 39.4%, respectively, which was solid phase at room temperature (See Table 17). When the temperature increased from 360 ˚C to 390 ˚C, conversions remained constant while diesel yield decreased because the higher temperature increasing the gasoline yield.

Gas product composition of CoMoC/Al and CoMoN/Al catalysts are shown in Figure 19b. High CH_4 gas composition in the hydrotreating temperature of 360 ˚C and 390 ˚C of CoMoC/Al due to the increase in cracking, isomerization, and cyclization reaction when the temperature is higher [70].

Liquid product composition and contribution of HDO and DCO_x are shown in Figure 19c. The increases in temperature, $\%DCO_x$ slightly increased the contribution of HDO and DCO_x for both catalysts (CoMoC/Al and CoMoN/Al). These results were consistent to previous studies as increase in temperature increased $\%DCO_x$ contribution [50], resulting from the endothermic DCO_x pathway. Therefore, the increased contribution of DCO_x, increasing the sum of CO, CO_2 and CH_4 in gas product composition (See Figure 19b).

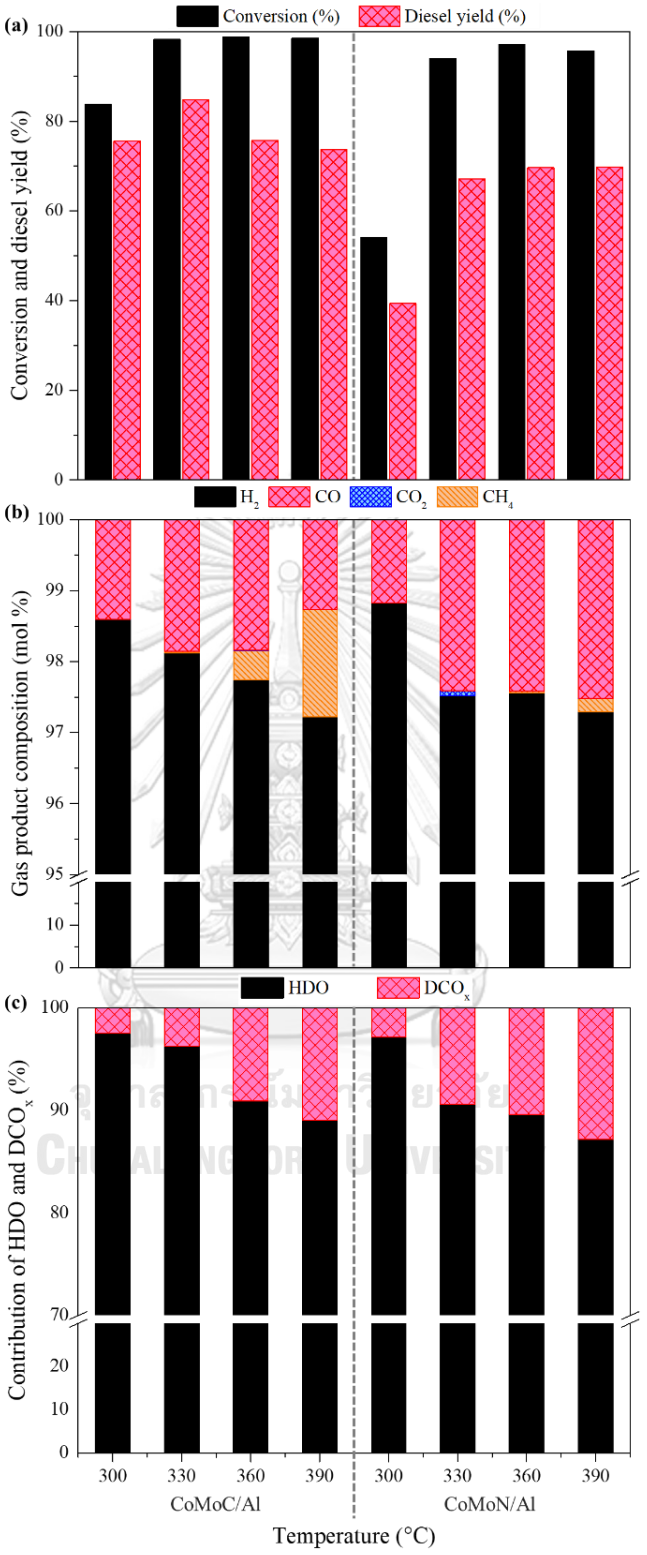

Figure 19 Effect of temperature of CoMoC/Al and CoMoN/Al catalysts on (a) conversion and diesel yield (b) gas product composition (c) contribution of HDO and DCO_x were performed at 5MPa of hydrogen pressure, 1 h^{-1} of LHSV and 1000 N($cm^3 \cdot cm^{-3}$) of H_2/feed ratio.

5.2.2 Effect of hydrogen pressure

The effect of the hydrogen pressure on the hydrotreating process was carried out over CoMoC/Al and CoMoN/Al catalysts in a continuous process. The pressure was studied at 3 MPa and 5 MPa under fixed 330 ˚C of temperature, 1 h^{-1} of LSHV, and 1000 N($cm^3 \cdot cm^{-3}$) of H_2/feed ratio.

The effect of hydrogen pressure of Como/Al and CoMoN/Al catalysts on conversion and diesel yield are shown in Figure 20a. The conversion, selectivity, yield, product phase and product color exhibits are summarized in Table 17. Conversion and diesel yield of CoMoC/Al and CoMoN/Al catalysts gradually decreased when decreasing hydrogen pressure from 5 MPa to 3 MPa. The CoMoC/Al catalyst showed higher diesel yield than CoMoN/Al catalyst at 3 MPa of hydrogen pressure, which diesel yield of CoMoC/Al and CoMoN/Al catalyst was 82.9% and 64.7%, respectively. At 5 MPa of hydrogen pressure, diesel yield of CoMoC/Al catalyst (84.8%) higher than CoMoN/Al catalyst (67.1%). This result indicates that the decrease of the pressure from 5 MPa to 3 MPa had a small effect on the catalyst activity.

The Effect of hydrogen pressure of CoMoC/Al and CoMoN/Al catalysts on gas product composition are shown in Figure 20b. Gas product compositions (Mixed of CO, CO_2 and CH_4 gas) of CoMoC/Al catalyst were approximate 1.8 mol%-1.9 mol%. Likewise, Gas product compositions (Mixed of CO, CO_2 and CH_4 gas) of CoMoN/Al catalyst were approximate 2.4 mol%-2.5 mol%. Besides, CO_2 gas at 3 MPa of hydrogen pressures is observed. As a result of the decreased hydrogen pressures from 5 MPa to 3 MPa with decreasing methanation (Side reaction of deoxygenation). Thus, CO_2 doesn't convert to CH_4 by methanation.

จุฬาลงกรณ์มหาวิทยาลัย
Chulalongkorn University

The Effect of hydrogen pressure of CoMoC/Al and CoMoN/Al catalysts on the contribution of HDO and DCO_x are shown in Figure 20c. Decreasing hydrogen pressure had not significant effect on the reaction pathway of deoxygenation at a temperature of 330 ˚C.

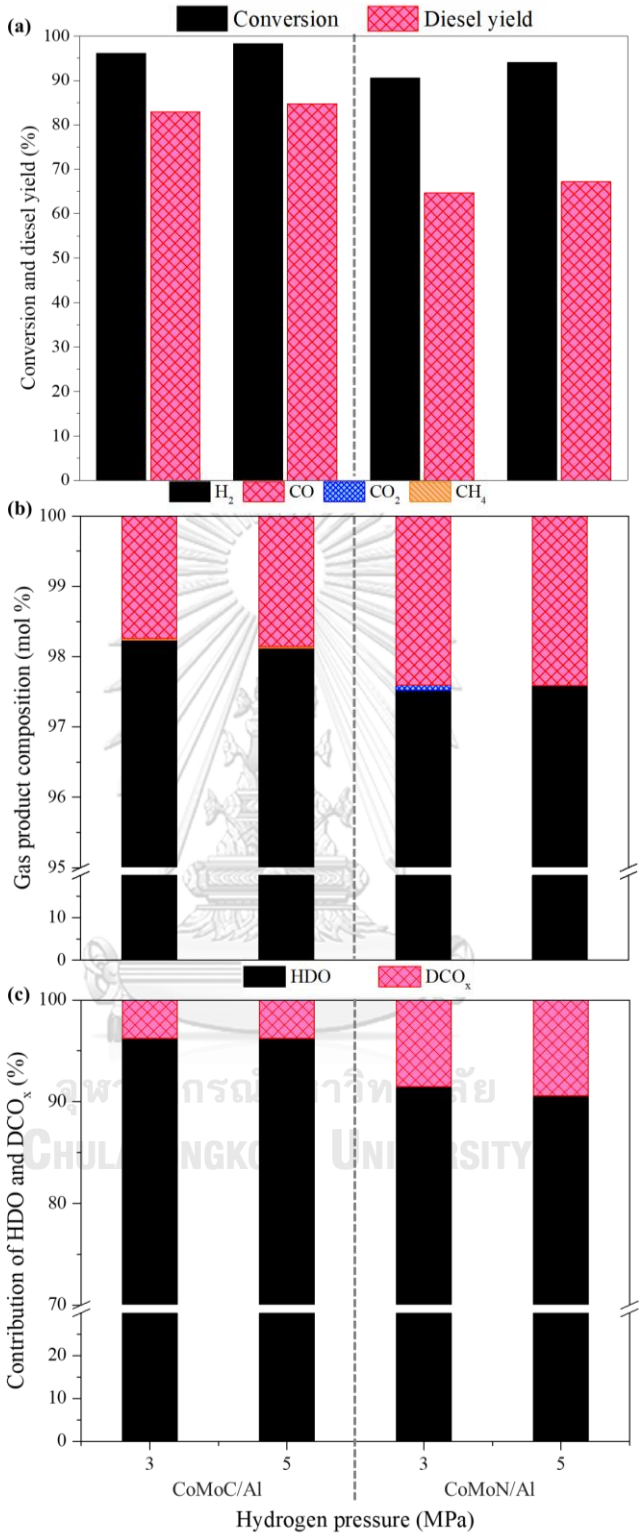

Figure 20 Effect of hydrogen pressure of CoMoC/Al and CoMoN/Al catalysts on (a) conversion and diesel yield (b) gas product composition (c) contribution of HDO and DCO_x were performed at 330 ˚C of temperature, 1 h^{-1} of LHSV and 1000 N($cm^3 \cdot cm^{-3}$) of H_2/feed ratio.

5.3 Stability of catalysts

From the result of catalysis screening and optimal operating conditions, CoMoC/Al and CoMoN/Al catalysts show high activity than other catalysts. The operating conditions at 330 ˚C of temperature and 5 MPa of hydrogen pressure were optimal operating parameter for catalytic deoxygenation. Therefore, in the section, the stability of CoMoC/Al and CoMoN/Al catalysts in deoxygenation of PFAD were studied in a trickle bed reactor at 330 ˚C of temperature, 5 MPa of hydrogen pressure, 1 h^{-1} LHSV and 1000 N($cm^3 \cdot cm^{-3}$) of H_2/feed ratio. The stability of CoMoC/Al and CoMoN/Al catalysts on PFAD conversion and diesel yield are shown in Figure 21. The PFAD conversion of CoMoC/Al catalyst remained constant to 72 h. and then decreased meanwhile, the PFAD conversion of CoMoN/Al catalyst remained constant to 18 h. and then decreased. In addition, the diesel yield of CoMoC/Al catalyst remained constant to 72 h. and then decreased slowly, but the diesel yield of CoMoN/Al catalyst significantly dropper after 6 h.

The TGA profiles of spent catalysts after the catalytic stability test are exhibited in Figure 22. The different weight loss between fresh and spent of CoMoC/Al and CoMoN/Al catalysts were 14.6% and 28.2%, respectively. Although the long-term reaction tests of CoMoC/Al catalysts were performed for 102 h. on-stream, the CoMoC/Al catalyst showed low weight loss, indicating high stability and low deactivation of CoMoC/Al catalyst in compared with CoMoN/Al catalyst.

จุฬาลงกรณ์มหาวิทยาลัย
Chulalongkorn University

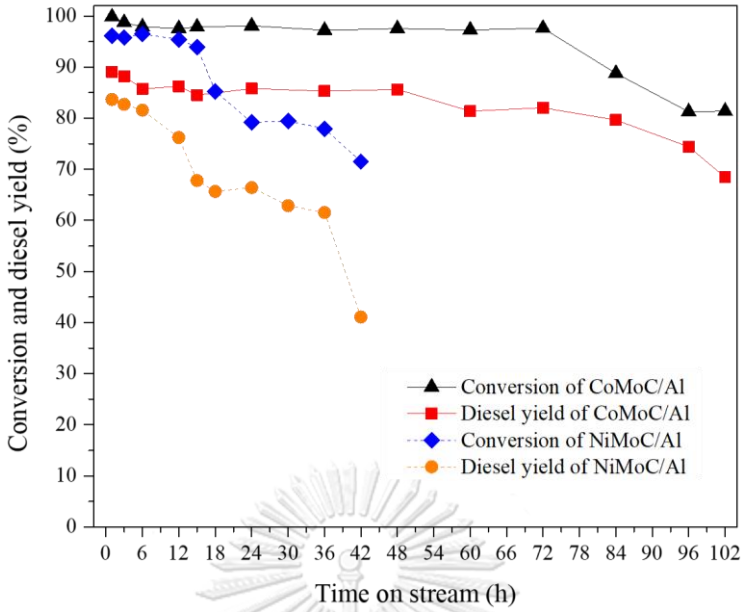

Figure 21 Catalytic stability test of CoMoC/Al and CoMoN/Al catalysts on conversion and diesel yield effect were performed at a temperature of 330 °C, 5 MPa of hydrogen pressure, 1 h^{-1} of LHSV and 1000 $N(cm^3 \cdot cm^{-3})$ of H_2/feed ratio.

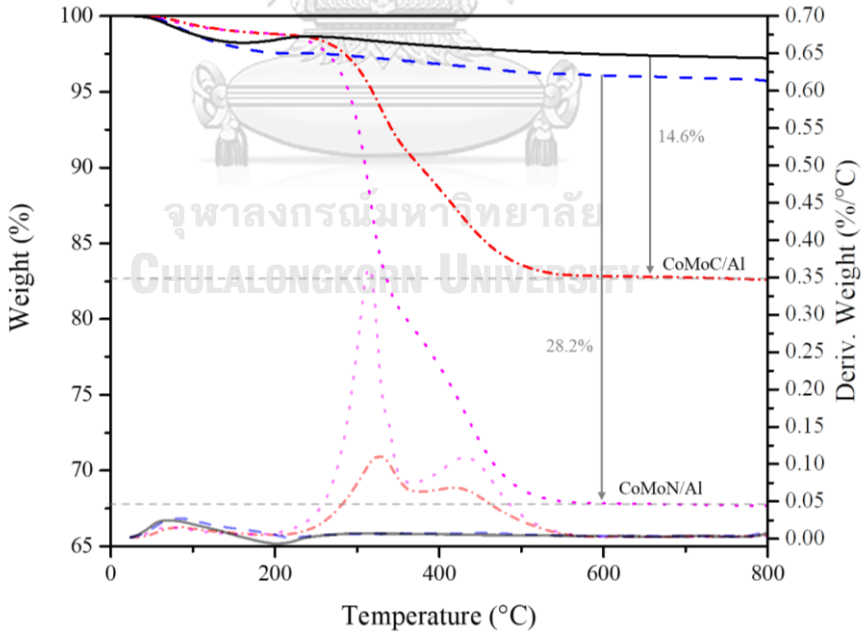

Figure 22 TG/DTG profiles of the fresh and spent catalysts on catalytic stability test. The operating condition at a temperature of 330 °C, 5 MPa of hydrogen pressure, 1 h^{-1} of LHSV and 1000 $N(cm^3 \cdot cm^{-3})$ of H_2/feed ratio.

CHAPTER VI

CONCLUSION

This work aims to produce green diesel from PFAD (palm fatty acid distillate, a residual from palm oil refinery) using transition metal and non-sulfide catalysts via deoxygenation in a trickle bed reactor. The Mo nitride-based catalysts were prepared by the single-step decomposition method, while the Mo carbide-based catalysts were prepared by the single-step decomposition and the temperature-programmed reduction method. The properties of catalysts were investigated by XRD, XPS, SEM/EDX, N_2-physisorption and TGA. The catalytic performance was evaluated considering PFAD conversion, diesel yield and contribution of HDO and DCO_x.

The catalyst performance was evaluated at a temperature of 330 °C, hydrogen pressure of 5 MPa, LHSV of 1 h^{-1}, and H_2/feed ratio of 1000 $Ncm^3 \cdot cm^{-3}$. It was found that the carbide catalysts exhibited the superior performance than those of nitride catalysts. The bimetallic CoMoC showed higher diesel yield than monometallic Mo carbide and bimetallic NiMoC catalysts. Thus, the CoMoC and NiMoC catalysts were selected for further investigations. The hydrodeoxygenation (HDO) is a dominant reaction pathway for all catalysts.

The catalysts prepared by a single-step decomposition method exhibited higher catalytic activity than that of the catalysts prepared by temperature-programmed reduction method due to higher catalyst surface area. Consequently, the single-step composition method is a good alternative for the preparation of a bimetallic carbide catalyst.

จุฬาลงกรณ์มหาวิทยาลัย
Chulalongkorn University

In order to optimize the operating conditions, the operating temperatures were varied from 300 to 390 °C under 3-5 MPa of hydrogen pressure. The operating temperature of 330 °C and 5 MPa of hydrogen pressure was found to be a suitable condition for CoMoC and NiMoC catalysts. The reaction temperature and hydrogen pressure have slight effects on reaction pathways.

In the stability test, the CoMoC catalyst exhibited complete PFAD conversion with a diesel yield of 82.0% for 72 h. time on stream. However, the catalytic activity of CoMoC catalyst gradually decreased after 72 h., and PFAD conversion of 81% with diesel yield of 68.5% were obtained after 102 h. time on stream.

REFERENCES

1. Lau, L.C., K.T. Lee, and A.R. Mohamed, *Global warming mitigation and renewable energy policy development from the Kyoto Protocol to the Copenhagen Accord—A comment.* Renewable and Sustainable Energy Reviews, 2012. **16**(7): p. 5280-5284.
2. Viner, K.J., H.M. Roy, R. Lee, O. He, P. Champagne, and P.G. Jessop, *Transesterification of soybean oil using a switchable-hydrophilicity solvent, 2-(dibutylamino) ethanol.* Green Chemistry, 2019. **21**(17): p. 4786-4791.
3. Wang, S., C. Zhao, R. Shan, Y. Wang, and H. Yuan, *A novel peat biochar supported catalyst for the transesterification reaction.* Energy conversion and management, 2017. **139**: p. 89-96.
4. Jung, J.-M., J. Lee, K.-H. Kim, S.R. Lee, H. Song, and E.E. Kwon, *Biodiesel conversion via thermal assisted in-situ transesterification of bovine fat using dimethyl carbonate as an acyl acceptor.* ACS Sustainable Chemistry & Engineering, 2016. **4**(10): p. 5600-5605.
5. Liu, Y., R. Sotelo-Boyás, K. Murata, T. Minowa, and K. Sakanishi, *Production of bio-hydrogenated diesel by hydrotreatment of high-acid-value waste cooking oil over ruthenium catalyst supported on Al-polyoxocation-pillared montmorillonite.* Catalysts, 2012. **2**(1): p. 171-190.
6. Zhou, L. and A. Lawal, *Hydrodeoxygenation of microalgae oil to green diesel over Pt, Rh and presulfided NiMo catalysts.* Catalysis Science & Technology, 2016. **6**(5): p. 1442-1454.
7. Sari, E., M. Kim, S.O. Salley, and K.S. Ng, *A highly active nanocomposite silica-carbon supported palladium catalyst for decarboxylation of free fatty acids for green diesel production: Correlation of activity and catalyst properties.* Applied Catalysis A: General, 2013. **467**: p. 261-269.
8. Alsultan, G.A., N. Asikin-Mijan, H. Lee, A.S. Albazzaz, and Y. Taufiq-Yap, *Deoxygenation of waste cooking to renewable diesel over walnut shell-derived nanorode activated carbon supported CaO-La2O3 catalyst.* Energy Conversion and Management, 2017. **151**: p. 311-323.
9. Liu, C., J. Liu, G. Zhou, W. Tian, and L. Rong, *A cleaner process for hydrocracking of jatropha oil into green diesel.* Journal of the Taiwan Institute of Chemical Engineers, 2013. **44**(2): p. 221-227.
10. Pongsiriyakul, K., W. Kiatkittipong, K. Kiatkittipong, N. Laosiripojana, K. Faungnawakij, S. Adhikari, and S. Assabumrungrat, *Alternative Hydrocarbon Biofuel Production via Hydrotreating under a Synthesis Gas Atmosphere.* Energy & Fuels, 2017. **31**(11): p. 12256-12262.
11. Heriyanto, H., S.M. Sumbogo, S.I. Heriyanti, I. Sholehah, and A. Rahmawati. *Synthesis of green diesel from waste cooking oil through hydrodeoxygenation technology with NiMo/γ-Al2O3 catalysts*. in *MATEC Web of Conferences*. 2018. EDP Sciences.
12. de Sousa, F.P., C.C. Cardoso, and V.M. Pasa, *Producing hydrocarbons for green diesel and jet fuel formulation from palm kernel fat over Pd/C.* Fuel processing technology, 2016. **143**: p. 35-42.
13. Phimsen, S., W. Kiatkittipong, H. Yamada, T. Tagawa, K. Kiatkittipong, N. Laosiripojana, and S. Assabumrungrat, *Oil extracted from spent coffee grounds*

for bio-hydrotreated diesel production. Energy Conversion and Management, 2016. **126**: p. 1028-1036.

14. Ameen, M., M.T. Azizan, A. Ramli, S. Yusup, and M.S. Alnarabiji, *Catalytic hydrodeoxygenation of rubber seed oil over sonochemically synthesized Ni-Mo/γ-Al2O3 catalyst for green diesel production.* Ultrasonics sonochemistry, 2019. **51**: p. 90-102.
15. Kiatkittipong, W., S. Phimsen, K. Kiatkittipong, S. Wongsakulphasatch, N. Laosiripojana, and S. Assabumrungrat, *Diesel-like hydrocarbon production from hydroprocessing of relevant refining palm oil.* Fuel processing technology, 2013. **116**: p. 16-26.
16. Ping, B.T.Y. and M. Yusof, *Characteristics and properties of fatty acid distillates from palm oil.* Oil Palm Bulletin, 2009. **59**: p. 5-11.
17. Vasquez, M.C., E.E. Silva, and E.F. Castillo, *Hydrotreatment of vegetable oils: A review of the technologies and its developments for jet biofuel production.* Biomass and Bioenergy, 2017. **105**: p. 197-206.
18. Li, X., X. Luo, Y. Jin, J. Li, H. Zhang, A. Zhang, and J. Xie, *Heterogeneous sulfur-free hydrodeoxygenation catalysts for selectively upgrading the renewable bio-oils to second generation biofuels.* Renewable and Sustainable Energy Reviews, 2018. **82**: p. 3762-3797.
19. Zhao, C., T. Brück, and J.A. Lercher, *Catalytic deoxygenation of microalgae oil to green hydrocarbons.* Green Chemistry, 2013. **15**(7): p. 1720-1739.
20. Boda, L., G. Onyestyák, H. Solt, F. Lónyi, J. Valyon, and A. Thernesz, *Catalytic hydroconversion of tricaprylin and caprylic acid as model reaction for biofuel production from triglycerides.* Applied Catalysis A: General, 2010. **374**(1-2): p. 158-169.
21. Huber, G.W., P. O'Connor, and A. Corma, *Processing biomass in conventional oil refineries: Production of high quality diesel by hydrotreating vegetable oils in heavy vacuum oil mixtures.* Applied Catalysis A: General, 2007. **329**: p. 120-129.
22. Marker, T.L., *Opportunities for biorenewables in oil refineries*. 2005, UOP LLC.
23. Imahara, H., E. Minami, and S. Saka, *Thermodynamic study on cloud point of biodiesel with its fatty acid composition.* Fuel, 2006. **85**(12-13): p. 1666-1670.
24. Manchanda, T., R. Tyagi, and D.K. Sharma, *Comparison of fuel characteristics of green (renewable) diesel with biodiesel obtainable from algal oil and vegetable oil.* Energy Sources, Part A: Recovery, Utilization, and Environmental Effects, 2018. **40**(1): p. 54-59.
25. Vonortas, A. and N. Papayannakos, *Comparative analysis of biodiesel versus green diesel.* Wiley Interdisciplinary Reviews: Energy and Environment, 2014. **3**(1): p. 3-23.
26. Walendziewski, J., M. Stolarski, R. Łużny, and B. Klimek, *Hydroprocesssing of light gas oil—rape oil mixtures.* Fuel Processing Technology, 2009. **90**(5): p. 686-691.
27. Guzman, A., J.E. Torres, L.P. Prada, and M.L. Nunez, *Hydroprocessing of crude palm oil at pilot plant scale.* Catalysis Today, 2010. **156**(1-2): p. 38-43.
28. Zambiazi, R.C., R. Przybylski, M.W. Zambiazi, and C.B. Mendonça, *Fatty acid composition of vegetable oils and fats.* Boletim do Centro de Pesquisa de

Processamento de Alimentos, 2007. **25**(1).
29. Hachemi, I., N. Kumar, P. Mäki-Arvela, J. Roine, M. Peurla, J. Hemming, J. Salonen, and D.Y. Murzin, *Sulfur-free Ni catalyst for production of green diesel by hydrodeoxygenation.* Journal of catalysis, 2017. **347**: p. 205-221.
30. Xin, H., K. Guo, D. Li, H. Yang, and C. Hu, *Production of high-grade diesel from palmitic acid over activated carbon-supported nickel phosphide catalysts.* Applied Catalysis B: Environmental, 2016. **187**: p. 375-385.
31. Baharudin, K.B., Y.H. Taufiq-Yap, J. Hunns, M. Isaacs, K. Wilson, and D. Derawi, *Mesoporous NiO/Al-SBA-15 catalysts for solvent-free deoxygenation of palm fatty acid distillate.* Microporous and Mesoporous Materials, 2019. **276**: p. 13-22.
32. Zhou, L. and A. Lawal, *Kinetic study of hydrodeoxygenation of palmitic acid as a model compound for microalgae oil over Pt/γ-Al2O3.* Applied Catalysis A: General, 2017. **532**: p. 40-49.
33. Stepacheva, A.A., L.Z. Nikoshvili, E.M. Sulman, and V.G. Matveeva, *Hydrodeoxygenation of stearic acid for the production of "green" diesel.* Green Processing and Synthesis, 2014. **3**(6): p. 441-446.
34. Kamaruzaman, M.F., Y.H. Taufiq-Yap, and D. Derawi, *Green diesel production from palm fatty acid distillate over SBA-15-supported nickel, cobalt, and nickel/cobalt catalysts.* Biomass and Bioenergy, 2020. **134**: p. 105476.
35. Ding, R., Y. Wu, Y. Chen, J. Liang, J. Liu, and M. Yang, *Effective hydrodeoxygenation of palmitic acid to diesel-like hydrocarbons over MoO2/CNTs catalyst.* Chemical Engineering Science, 2015. **135**: p. 517-525.
36. Hollak, S.A., R.W. Gosselink, D.S. van Es, and J.H. Bitter, *Comparison of tungsten and molybdenum carbide catalysts for the hydrodeoxygenation of oleic acid.* Acs Catalysis, 2013. **3**(12): p. 2837-2844.
37. Lestari, S., P. Mäki-Arvela, I. Simakova, J. Beltramini, G.M. Lu, and D.Y. Murzin, *Catalytic deoxygenation of stearic acid and palmitic acid in semibatch mode.* Catalysis Letters, 2009. **130**(1-2): p. 48-51.
38. Srifa, A., K. Faungnawakij, V. Itthibenchapong, N. Viriya-Empikul, T. Charinpanitkul, and S. Assabumrungrat, *Production of bio-hydrogenated diesel by catalytic hydrotreating of palm oil over NiMoS2/γ-Al2O3 catalyst.* Bioresource technology, 2014. **158**: p. 81-90.
39. Yang, Y., Q. Wang, X. Zhang, L. Wang, and G. Li, *Hydrotreating of C18 fatty acids to hydrocarbons on sulphided NiW/SiO2–Al2O3.* Fuel processing technology, 2013. **116**: p. 165-174.
40. Toba, M., Y. Abe, H. Kuramochi, M. Osako, T. Mochizuki, and Y. Yoshimura, *Hydrodeoxygenation of waste vegetable oil over sulfide catalysts.* Catalysis Today, 2011. **164**(1): p. 533-537.
41. Srifa, A., K. Faungnawakij, V. Itthibenchapong, and S. Assabumrungrat, *Roles of monometallic catalysts in hydrodeoxygenation of palm oil to green diesel.* Chemical Engineering Journal, 2015. **278**: p. 249-258.
42. Snåre, M., I. Kubicˇkova, P. Mäki-Arvela, K. Eränen, and D.Y. Murzin, *Heterogeneous catalytic deoxygenation of stearic acid for production of biodiesel.* Industrial & engineering chemistry research, 2006. **45**(16): p. 5708-5715.
43. Monnier, J., H. Sulimma, A. Dalai, and G. Caravaggio, *Hydrodeoxygenation of*

oleic acid and canola oil over alumina-supported metal nitrides. Applied Catalysis A: General, 2010. **382**(2): p. 176-180.

44. Wang, F., J. Jiang, K. Wang, Q. Zhai, H. Sun, P. Liu, J. Feng, H. Xia, J. Ye, and Z. Li, *Activated carbon supported molybdenum and tungsten carbides for hydrotreatment of fatty acids into green diesel.* Fuel, 2018. **228**: p. 103-111.
45. Al Alwan, B., S.O. Salley, and K.S. Ng, *Hydrocracking of DDGS corn oil over transition metal carbides supported on Al-SBA-15: Effect of fractional sum of metal electronegativities.* Applied Catalysis A: General, 2014. **485**: p. 58-66.
46. Kim, S.K., D. Yoon, S.-C. Lee, and J. Kim, *Mo2C/graphene nanocomposite as a hydrodeoxygenation catalyst for the production of diesel range hydrocarbons.* Acs Catalysis, 2015. **5**(6): p. 3292-3303.
47. Wang, H., S. Yan, S.O. Salley, and K.S. Ng, *Support effects on hydrotreating of soybean oil over NiMo carbide catalyst.* Fuel, 2013. **111**: p. 81-87.
48. Kumar, P., S.R. Yenumala, S.K. Maity, and D. Shee, *Kinetics of hydrodeoxygenation of stearic acid using supported nickel catalysts: Effects of supports.* Applied Catalysis A: General, 2014. **471**: p. 28-38.
49. Palcheva, R., L. KALUŽA, A. Spojakina, K. JIRÁTOVÁ, and G. Tyuliev, *NiMo/γ-Al2O3 catalysts from ni heteropolyoxomolybdate and effect of alumina modification by b, co, or ni.* Chinese Journal of Catalysis, 2012. **33**(4-6): p. 952-961.
50. Taromi, A.A. and S. Kaliaguine, *Green diesel production via continuous hydrotreatment of triglycerides over mesostructured γ-alumina supported NiMo/CoMo catalysts.* Fuel processing technology, 2018. **171**: p. 20-30.
51. Fu, X., H. Su, W. Yin, Y. Huang, and X. Gu, *Bimetallic molybdenum nitride Co 3 Mo 3 N: a new promising catalyst for CO 2 reforming of methane.* Catalysis Science & Technology, 2017. **7**(8): p. 1671-1678.
52. Aegerter, P.A., W.W. Quigley, G.J. Simpson, D.D. Ziegler, J.W. Logan, K.R. McCrea, S. Glazier, and M.E. Bussell, *Thiophene hydrodesulfurization over alumina-supported molybdenum carbide and nitride catalysts: adsorption sites, catalytic activities, and nature of the active surface.* Journal of Catalysis, 1996. **164**(1): p. 109-121.
53. Korlann, S., B. Diaz, and M.E. Bussell, *Synthesis of bulk and alumina-supported bimetallic carbide and nitride catalysts.* Chemistry of materials, 2002. **14**(10): p. 4049-4058.
54. Guo, L., J. Wang, X. Teng, Y. Liu, X. He, and Z. Chen, *A Novel Bimetallic Nickel–Molybdenum Carbide Nanowire Array for Efficient Hydrogen Evolution.* ChemSusChem, 2018. **11**(16): p. 2717-2723.
55. Zhao, L., K. Fang, D. Jiang, D. Li, and Y. Sun, *Sol–gel derived Ni–Mo bimetallic carbide catalysts and their performance for CO hydrogenation.* Catalysis Today, 2010. **158**(3-4): p. 490-495.
56. Qiu, L., L. Jiang, Z. Ye, Y. Liu, T. Cen, X. Peng, and D. Yuan, *Phosphorus-doped Co3Mo3C/Co/CNFs hybrid: A remarkable electrocatalyst for hydrogen evolution reaction.* Electrochimica Acta, 2019. **325**: p. 134962.
57. Shi, C., A. Zhang, X. Li, S. Zhang, A. Zhu, Y. Ma, and C. Au, *Ni-modified Mo2C catalysts for methane dry reforming.* Applied Catalysis A: General, 2012. **431**: p. 164-170.
58. Yang, H., J. Liu, J. Wang, C.K. Poh, W. Zhou, J. Lin, and Z. Shen,

Electrocatalytically active graphene supported MMo carbides (MNi, Co) for oxygen reduction reaction. Electrochimica Acta, 2016. **216**: p. 246-252.

59. Thongkumkoon, S., W. Kiatkittipong, U.W. Hartley, N. Laosiripojana, and P. Daorattanachai, *Catalytic activity of trimetallic sulfided Re-Ni-Mo/γ-Al2O3 toward deoxygenation of palm feedstocks.* Renewable Energy, 2019. **140**: p. 111-123.
60. Chen, S., G. Zhou, H. Xie, Z. Jiao, and X. Zhang, *Hydrodeoxygenation of methyl laurate over the sulfur-free Ni/γ-Al2O3 catalysts.* Applied Catalysis A: General, 2019. **569**: p. 35-44.
61. Zhang, Z., Y. Tian, L. Zhang, S. Hu, J. Xiang, Y. Wang, L. Xu, Q. Liu, S. Zhang, and X. Hu, *Impacts of nickel loading on properties, catalytic behaviors of Ni/geAl2O3 catalysts and the reaction intermediates formed in methanation of CO2.* international journal of hydrogen energy, 2019. **44**(9291): p. e9306.
62. Wang, X.-H., M.-H. Zhang, W. Li, and K.-Y. Tao, *A simple synthesis route and characterisation of Co 3 Mo 3 C.* Dalton Transactions, 2007(44): p. 5165-5170.
63. Wang, X.-H., M.-H. Zhang, W. Li, and K.-Y. Tao, *Synthesis and characterization of cobalt–molybdenum bimetallic carbides catalysts.* Catalysis today, 2008. **131**(1-4): p. 111-117.
64. Li, Y., C. Zhang, Y. Liu, X. Hou, R. Zhang, and X. Tang, *Coke deposition on Ni/HZSM-5 in bio-oil hydrodeoxygenation processing.* Energy & Fuels, 2015. **29**(3): p. 1722-1728.
65. Akhmetzyanova, U., Z. Tišler, N. Sharkov, L. Skuhrovcová, L. Pelíšková, O. Kikhtyanin, P. Mäki-Arvela, M. Opanasenko, M. Peurla, and D.Y. Murzin, *Molybdenum Nitrides, Carbides and Phosphides as Highly Efficient Catalysts for the (hydro) Deoxygenation Reaction.* ChemistrySelect, 2019. **4**(29): p. 8453-8459.
66. Carmona, H.D.P., J. Horáček, Z. Tišler, and U. Akhmetzyanova, *Sulfur free supported MoCx and MoNx catalysts for the hydrotreatment of atmospheric gasoil and its blends with rapeseed oil.* Fuel, 2019. **254**: p. 115582.
67. Arun, N., J. Maley, N. Chen, R. Sammynaiken, Y. Hu, and A.K. Dalai, *NiMo nitride supported on γ-Al2O3 for hydrodeoxygenation of oleic acid: Novel characterization and activity study.* Catalysis Today, 2017. **291**: p. 153-159.
68. Tominaga, H., Y. Aoki, and M. Nagai, *Hydrogenation of CO on molybdenum and cobalt molybdenum carbides.* Applied Catalysis A: General, 2012. **423**: p. 192-204.
69. Mahboubifar, M., S. Yousefinejad, M. Alizadeh, and B. Hemmateenejad, *Prediction of the acid value, peroxide value and the percentage of some fatty acids in edible oils during long heating time by chemometrics analysis of FTIR-ATR spectra.* Journal of the Iranian Chemical Society, 2016. **13**(12): p. 2291-2299.
70. Srifa, A. and S. Assabumrungrat, *DEOXYGENATION OF PALM OIL TO BIO-HYDROGENATED DIESEL OVER METAL AND METAL SULFIDE CATALYSTS IN A TRICKLE-BED REACTOR*. 2014, Chulalongkorn University.

APPENDIX

จุฬาลงกรณ์มหาวิทยาลัย
CHULALONGKORN UNIVERSITY

APPENDIX A
CALCULATIONS FOR CATALYSTS PREPARATION

Table A.1 Chemicals of properties

Component	Molecular weight	Precursor	Molecular weight	Purity (%)
Mo	95.95	$(NH_4)_6Mo_7O_{24}\bullet 4H_2O$	1235.86	81-83
Ni	58.69	$Ni(NO_3)_2\bullet 6H_2O$	290.81	97
Co	58.93	$Co(NO_3)_2\bullet 6H_2O$	291.03	100
-	-	$N_4(CH_2)_6$	140.19	-

A.1 The single-step decomposition method.

A.1.1 Impregnation of a mixture containing hexamethylenetetramine (HMTA): Preparation of 20%Mo on 2 g. γ-Al_2O_3 supported catalysts

$(NH_4)_6Mo_7O_{24}\cdot 4H_2O$ used precursor =

$$(2\ \text{g}\ \gamma-\text{Al}_2\text{O}_3)\left(\frac{20\ \text{g Mo}}{80\ \text{g}\ \gamma-\text{Al}_2\text{O}_3}\right)\left(\frac{1\ \text{mol Mo}}{95.95\ \text{g Mo}}\right)\left(\frac{1\text{mol}(\text{NH}_4)6\text{Mo}_7\text{O}_{24}\cdot 4\text{H}_2\text{O}}{7\ \text{mol Mo}}\right)$$
$$\times\left(\frac{1235.86\ \text{g}\ (\text{NH}_4)6\text{Mo}_7\text{O}_{24}\cdot 4\text{H}_2\text{O}}{1\ \text{mol}\ (\text{NH}_4)6\text{Mo}_7\text{O}_{24}\cdot 4\text{H}_2\text{O}}\right)\left(\frac{1}{0.82}\right)$$

$(NH_4)_6Mo_7O_{24}\cdot 4H_2O$ used precursor = 7.4436×10^{-4} mole
$(NH_4)_6Mo_7O_{24}\cdot 4H_2O$ used precursor = 1.1220 g

Base on $N_4(CH_2)_6$ (HMT): $(NH_4)_6Mo_7O_{24}\cdot 4H_2O$ = 2: 1 of mol ratio

$N_4(CH_2)_6$ (HMT) used precursor =

$$\left(7.4436\ \times\ 10^{-4}\ \text{mol}\ (\text{NH}_4)6\text{Mo}_7\text{O}_{24}\cdot 4\text{H}_2\text{O}\right)\left(\frac{2\ \text{mol HMT}}{1\ mol\ (\text{NH}_4)6\text{Mo}_7\text{O}_{24}\cdot 4\text{H}_2\text{O}}\right)$$
$$\times\left(\frac{140.19\ \text{g HMT}}{1\ \text{mol HMT}}\right)$$

$N_4(CH_2)_6$ (HMT) used precursor = 0.2087 g

A.1.2 Impregnation of a mixture containing hexamethylenetetramine (HMTA): Preparation of 20%CoMo on 2 g. γ-Al_2O_3 supported catalysts

$(NH_4)_6Mo_7O_{24}\cdot 4H_2O$ used precursor =

$$(2\ \mathrm{g}\ \gamma-\mathrm{Al_2O_3})\left(\frac{20\ \mathrm{g\ Mo\ and\ Co}}{80\ \mathrm{g}\ \gamma-\mathrm{Al_2O_3}}\right)\left(\frac{95.95\ \mathrm{g\ Mo}}{154.88\ \mathrm{g\ Mo\ and\ Co}}\right)\left(\frac{1\ \mathrm{mol\ Mo}}{95.95\ \mathrm{g\ Mo}}\right)$$
$$\times\left(\frac{1\ \mathrm{mol}\ (NH_4)6Mo_7O_{24}\cdot 4H_2O}{7\ \mathrm{mol\ Mo}}\right)\left(\frac{1235.86\ \mathrm{g}\ (NH_4)6Mo_7O_{24}\cdot 4H_2O}{1\ \mathrm{mol}\ (NH_4)6Mo_7O_{24}\cdot 4H_2O}\right)\left(\frac{1}{0.82}\right)$$

$(NH_4)_6Mo_7O_{24}\cdot 4H_2O$ used precursor = 4.6119×10^{-4} mole
$(NH_4)_6Mo_7O_{24}\cdot 4H_2O$ used precursor = 0.6951 g

$Co(NO_3)_2\bullet\ 6H_2O$ used precursor =

$$(2\ \mathrm{g}\ \gamma-\mathrm{Al_2O_3})\left(\frac{20\ \mathrm{g\ Mo\ and\ Co}}{80\ \mathrm{g}\ \gamma-\mathrm{Al_2O_3}}\right)\left(\frac{58.93\ \mathrm{g\ Co}}{154.88\ \mathrm{g\ Mo\ and\ Co}}\right)\left(\frac{1\ \mathrm{mol\ Co}}{58.93\ \mathrm{g\ Co}}\right)$$
$$\times\left(\frac{1\ \mathrm{mol}\ Co(NO_3)_2\cdot 6H_2O}{1\ \mathrm{mol\ Co}}\right)\left(\frac{291.03\ \mathrm{g}\ Co(NO_3)_2\cdot 6H_2O}{1\ \mathrm{mol}\ Co(NO_3)_2\cdot 6H_2O}\right)$$

$Co(NO_3)_2\bullet\ 6H_2O$ used precursor = 3.2283×10^{-3} mole
$Co(NO_3)_2\bullet\ 6H_2O$ used precursor = 0.9403 g

Base on $N_4(CH_2)_6$ (HMT): $(NH_4)_6Mo_7O_{24}\cdot 4H_2O$: $Co(NO_3)_2\bullet\ 6H_2O$ = 34: 2: 14 of mol ratio

$N_4(CH_2)_6$ (HMT) used precursor =

$$(4.6119\ \times\ 10^{-4}\ \mathrm{mol}\ (NH_4)6Mo_7O_{24}\cdot 4H_2O)\left(\frac{34\ \mathrm{mol\ HMT}}{2\ \mathrm{mol}\ (NH_4)6Mo_7O_{24}\cdot 4H_2O}\right)$$
$$\times\left(\frac{140.19\ \mathrm{g\ HMT}}{1\ \mathrm{mol\ HMT}}\right)$$

$N_4(CH_2)_6$ (HMT) used precursor = 1.1010 g

จุฬาลงกรณ์มหาวิทยาลัย
Chulalongkorn University

A.1.3 Impregnation of a mixture containing hexamethylenetetramine (HMTA): Preparation of 20%NiMo on 2 g. γ-Al_2O_3 supported catalysts

$(NH_4)_6Mo_7O_{24}\cdot 4H_2O$ used precursor =

$$(2\ \mathrm{g}\ \gamma-\mathrm{Al_2O_3})\left(\frac{20\ \mathrm{g\ Mo\ and\ Ni}}{80\ \mathrm{g}\ \gamma-\mathrm{Al_2O_3}}\right)\left(\frac{95.95\ \mathrm{g\ Mo}}{154.64\ \mathrm{g\ Mo\ and\ Ni}}\right)\left(\frac{1\ \mathrm{mol\ Mo}}{95.95\ \mathrm{g\ Mo}}\right)$$
$$\times\left(\frac{1\ \mathrm{mol}\ (\mathrm{NH_4})_6\mathrm{Mo_7O_{24}}\cdot 4\mathrm{H_2O}}{7\ \mathrm{mol\ Mo}}\right)\left(\frac{1235.86\ \mathrm{g}\ (\mathrm{NH_4})_6\mathrm{Mo_7O_{24}}\cdot 4\mathrm{H_2O}}{1\ \mathrm{mol}\ (\mathrm{NH_4})_6\mathrm{Mo_7O_{24}}\cdot 4\mathrm{H_2O}}\right)\left(\frac{1}{0.82}\right)$$

$(NH_4)_6Mo_7O_{24}\cdot 4H_2O$ used precursor = 4.6190×10^{-4} mole
$(NH_4)_6Mo_7O_{24}\cdot 4H_2O$ used precursor = 0.6962 g

$Ni(NO_3)_2\bullet\ 6H_2O$ used precursor =

$$(2\ \mathrm{g}\ \gamma-\mathrm{Al_2O_3})\left(\frac{20\ \mathrm{g\ Mo\ and\ Ni}}{80\ \mathrm{g}\ \gamma-\mathrm{Al_2O_3}}\right)\left(\frac{58.69\ \mathrm{g\ Ni}}{154.64\ \mathrm{g\ Mo\ and\ Ni}}\right)\left(\frac{1\ \mathrm{mol\ Ni}}{58.69\ \mathrm{g\ Ni}}\right)$$
$$\times\left(\frac{1\ \mathrm{mol\ Ni(NO_3)_2}\cdot 6\mathrm{H_2O}}{1\ \mathrm{mol\ Ni}}\right)\left(\frac{290.81\ \mathrm{g\ Ni(NO_3)_2}\cdot 6\mathrm{H_2O}}{1\ \mathrm{mol\ Ni(NO_3)_2}\cdot 6\mathrm{H_2O}}\right)\left(\frac{1}{0.97}\right)$$

$Ni(NO_3)_2\bullet\ 6H_2O$ used precursor = 3.2185×10^{-3} mole
$Ni(NO_3)_2\bullet\ 6H_2O$ used precursor = 0.9650 g

Base on $N_4(CH_2)_6$ (HMT): $(NH_4)_6Mo_7O_{24}\cdot 4H_2O$: $Co(NO_3)_2\bullet\ 6H_2O$ = 34: 2: 14 of mol ratio

$N_4(CH_2)_6$ (HMT) used precursor =

$$(4.6190\ \times\ 10^{-4}\ \mathrm{mol}\ (\mathrm{NH_4})_6\mathrm{Mo_7O_{24}}\cdot 4\mathrm{H_2O})\left(\frac{34\ \mathrm{mol\ HMT}}{2\ \mathrm{mol}\ (\mathrm{NH_4})_6\mathrm{Mo_7O_{24}}\cdot 4\mathrm{H_2O}}\right)$$
$$\times\left(\frac{140.19\ \mathrm{g\ HMT}}{1\ \mathrm{mol\ HMT}}\right)$$

$N_4(CH_2)_6$ (HMT) used precursor = 1.1008 g

จุฬาลงกรณ์มหาวิทยาลัย
Chulalongkorn University

A.2 The temperature-programmed reduction method (TPR).

A.2.1 Impregnation: Preparation of 20%CoMo on 2 g. γ-Al_2O_3 supported catalysts

$(NH_4)_6Mo_7O_{24}\cdot 4H_2O$ used precursor =

$$(2\ \mathrm{g}\ \gamma - Al_2O_3)\left(\frac{20\ \mathrm{g\ Mo\ and\ Co}}{80\ \mathrm{g}\ \gamma - Al_2O_3}\right)\left(\frac{95.95\ \mathrm{g\ Mo}}{154.88\ \mathrm{g\ Mo\ and\ Co}}\right)\left(\frac{1\ \mathrm{mol\ Mo}}{95.95\ \mathrm{g\ Mo}}\right)$$
$$\times\left(\frac{1\ \mathrm{mol}\ (NH_4)6Mo_7O_{24}\cdot 4H_2O}{7\ \mathrm{mol\ Mo}}\right)\left(\frac{1235.86\ \mathrm{g}\ (NH_4)6Mo_7O_{24}\cdot 4H_2O}{1\ \mathrm{mol}\ (NH_4)6Mo_7O_{24}\cdot 4H_2O}\right)\left(\frac{1}{0.82}\right)$$

$(NH_4)_6Mo_7O_{24}\cdot 4H_2O$ used precursor = 0.6951 g

$Co(NO_3)_2\bullet\ 6H_2O$ used precursor =

$$(2\ \mathrm{g}\ \gamma - Al_2O_3)\left(\frac{20\ \mathrm{g\ Mo\ and\ Co}}{80\ \mathrm{g}\ \gamma - Al_2O_3}\right)\left(\frac{58.93\ \mathrm{g\ Co}}{154.88\ \mathrm{g\ Mo\ and\ Co}}\right)\left(\frac{1\ \mathrm{mol\ Co}}{58.93\ \mathrm{g\ Co}}\right)$$
$$\times\left(\frac{1\ \mathrm{mol}\ Co(NO_3)_2\cdot 6H_2O}{1\ \mathrm{mol\ Co}}\right)\left(\frac{291.03\ \mathrm{g}\ Co(NO_3)_2\cdot 6H_2O}{1\ \mathrm{mol}\ Co(NO_3)_2\cdot 6H_2O}\right)$$

$Co(NO_3)_2\bullet\ 6H_2O$ used precursor = 0.9403 g

จุฬาลงกรณ์มหาวิทยาลัย
Chulalongkorn University

A.2.2 Impregnation: Preparation of 20%NiMo on 2 g. γ-Al_2O_3 supported catalysts

$(NH_4)_6Mo_7O_{24}\cdot 4H_2O$ used precursor =

$$(2\ \mathrm{g}\ \gamma - Al_2O_3)\left(\frac{20\ \mathrm{g\ Mo\ and\ Ni}}{80\ \mathrm{g}\ \gamma - Al_2O_3}\right)\left(\frac{95.95\ \mathrm{g\ Mo}}{154.64\ \mathrm{g\ Mo\ and\ Ni}}\right)\left(\frac{1\ \mathrm{mol\ Mo}}{95.95\ \mathrm{g\ Mo}}\right)$$
$$\times\left(\frac{1\ \mathrm{mol}\ (NH_4)_6Mo_7O_{24}\cdot 4H_2O}{7\ \mathrm{mol\ Mo}}\right)\left(\frac{1235.86\ \mathrm{g}\ (NH_4)_6Mo_7O_{24}\cdot 4H_2O}{1\ \mathrm{mol}\ (NH_4)_6Mo_7O_{24}\cdot 4H_2O}\right)\left(\frac{1}{0.82}\right)$$

$(NH_4)_6Mo_7O_{24}\cdot 4H_2O$ used precursor = 4.6190×10^{-4} mole
$(NH_4)_6Mo_7O_{24}\cdot 4H_2O$ used precursor = 0.6962 g

$Ni(NO_3)_2\bullet\ 6H_2O$ used precursor =

$$(2\ \mathrm{g}\ \gamma - Al_2O_3)\left(\frac{20\ \mathrm{g\ Mo\ and}\ Ni}{80\ \mathrm{g}\ \gamma - Al_2O_3}\right)\left(\frac{58.69\ \mathrm{g\ Ni}}{154.64\ \mathrm{g\ Mo\ and\ Ni}}\right)\left(\frac{1\ \mathrm{mol\ Ni}}{58.69\ \mathrm{g\ Ni}}\right)$$
$$\times\left(\frac{1\ \mathrm{mol\ Ni}(NO_3)_2\cdot 6H_2O}{1\ \mathrm{mol}\ Ni}\right)\left(\frac{290.81\ \mathrm{g\ Ni}(NO_3)_2\cdot 6H_2O}{1\ \mathrm{mol\ Ni}(NO_3)_2\cdot 6H_2O}\right)\left(\frac{1}{0.97}\right)$$

$Ni(NO_3)_2\bullet\ 6H_2O$ used precursor = 3.2185×10^{-3} mole
$Ni(NO_3)_2\bullet\ 6H_2O$ used precursor = 0.9650 g

จุฬาลงกรณ์มหาวิทยาลัย
Chulalongkorn University

APPENDIX B
EXPERIMENTAL RAW DATA

Table B.1 Effect of catalysts on liquid product composition and % HDO and DCO_x contribution.

Catalysts	Liquid product composition (wt.%)					HDO (%)	DCO_x (%)
	n-C_{14}	n-C_{15}	n-C_{16}	n-C_{17}	n-C_{18}		
MoC/Al	0.8	1.1	31.5	1.6	21.5	95.3	4.7
MoN/Al	0.3	3.0	11.1	2.8	15.0	81.9	18.1
CoMoC/Al	1.3	1.5	42.4	1.6	37.8	96.2	3.8
CoMoN/Al	1.2	3.5	34.3	2.8	25.3	90.6	9.4
NiMoC/Al	0.8	5.1	26.1	6.2	29.6	83.4	16.6
NiMoN/Al	0.8	1.7	29.3	2.1	27.9	93.9	6.1

Table B.2 Effect of preparation method for bimetallic carbide catalysts on liquid product composition and % HDO and DCO_x contribution.

Catalysts	Liquid product composition (wt.%)					HDO (%)	DCO_x (%)
	n-C_{14}	n-C_{15}	n-C_{16}	n-C_{17}	n-C_{18}		
CoMoC/Al	1.3	1.5	42.4	1.6	37.8	96.2	3.8
CoMoC/Al-TPR	1.2	1.1	38.1	1.2	38.0	97.04	2.96
NiMoC/Al	0.8	5.1	26.1	6.2	29.6	83.4	16.6
NiMoC/Al-TPR	0.9	4.0	30.2	4.9	34.0	87.90	12.10

จุฬาลงกรณ์มหาวิทยาลัย
Chulalongkorn University

Table B.3 Effect of operating parameter on liquid product composition and % HDO and DCO_x contribution.

Catalysts	Parameter	Temperature (˚C)	Pressure (MPa)	Liquid product (wt.%)					HDO (%)	DCO_x (%)
				n-C14	n-C15	n-C16	n-C17	n-C18		
CoMoC/Al	Temperature	300	5	1.2	1.1	38.8	0.8	33.7	97.5	2.5
		330	5	1.3	1.5	42.4	1.6	37.8	90.9	9.1
		360	5	1.4	3.7	37.6	3.2	29.7	89.0	11.0
		390	5	1.6	4.3	37.3	3.8	26.7	89.6	10.4
	Pressure	330	3	1.3	1.5	41.6	1.6	36.9	96.2	3.8
		330	5	1.3	1.5	42.4	1.6	37.8	96.2	3.8
CoMoN/Al	Temperature	300	5	0.7	0.6	23.3	0.5	14.3	87.2	12.8
		330	5	1.2	3.5	34.3	2.8	25.3	97.1	2.9
		360	5	1.4	3.7	34.5	3.6	26.6	97.0	3.0
		390	5	1.5	4.9	35.0	4.1	24.4	87.9	12.1
	Pressure	330	3	1.0	2.6	34.7	2.9	23.4	91.5	8.5
		330	5	1.2	3.5	34.3	2.8	25.3	90.6	9.4

Table B.4 Liquid product composition and % HDO and DCO_x contribution of CoMoC/Al catalyst on stability test.

Time on stream (h)	Liquid product (wt.%)					HDO (%)	DCO_x (%)
	n-C14	n-C15	n-C16	n-C17	n-C18		
1	1.8	1.1	44.5	1.3	40.4	97.3	2.7
3	1.3	0.8	42.8	1.0	42.3	97.9	2.1
6	1.3	0.7	42.0	0.9	40.9	98.1	1.9
12	1.3	1.1	42.3	1.2	40.4	97.4	2.6
15	1.3	1.3	41.7	1.3	38.9	97.0	3.0
24	1.4	1.6	42.6	1.6	38.7	96.3	3.7
36	1.4	1.8	42.8	1.8	37.6	95.8	4.2
48	1.4	2.7	42.8	2.5	36.2	93.9	6.1
60	1.3	3.4	39.9	3.0	33.7	92.2	7.8
72	1.4	3.4	40.2	3.0	34.1	92.1	7.9
84	1.3	2.5	42.2	1.9	31.7	94.4	5.6
96	1.2	3.1	39.7	2.1	28.3	93.0	7.0
102	1.1	2.9	36.1	2.1	26.3	92.7	7.3

จุฬาลงกรณ์มหาวิทยาลัย Chulalongkorn University

Table B.5 Liquid product composition and % HDO and DCO_x contribution of CoMoN/Al catalyst on stability test.

Time on stream (h)	Liquid product (wt.%)					HDO (%)	DCO_x (%)
	n-C14	n-C15	n-C16	n-C17	n-C18		
1	1.4	3.0	40.1	3.1	36.2	92.8	7.2
3	1.3	2.7	39.6	2.8	36.4	93.4	6.6
6	1.4	3.0	40.4	2.8	34.0	92.9	7.1
12	1.1	3.0	38.7	2.8	30.7	92.5	7.5
15	1.0	2.6	35.9	2.4	25.9	92.6	7.4
18	1.3	2.6	34.0	2.9	25.0	91.7	8.3
24	1.6	3.0	34.6	2.7	24.5	91.5	8.5
30	1.1	3.0	33.8	2.2	22.9	91.7	8.3
36	1.1	3.4	32.7	2.4	21.9	90.6	9.4
42	0.7	2.7	21.9	1.8	13.9	89.0	11.0

จุฬาลงกรณ์มหาวิทยาลัย Chulalongkorn University

Table B.6 Effect of time on stream for CoMoC/Al catalyst on conversion, selectivity, yield, product phase and product color.

Time on stream (h)	Conversion (%)	Selectivity (%)		Yield (%)		Product phase	Product color
		Diesel selectivity	Gasoline selectivity	Diesel yield	Gasoline yield		
1	99.8	99.2	0.8	89.1	0.7	Liquid	Clear
3	98.8	99.5	0.5	88.2	0.4	Liquid	Clear
6	97.9	99.5	0.5	85.8	0.4	Liquid	Clear
12	97.6	99.4	0.6	86.3	0.5	Liquid	Clear
15	97.9	99.4	0.6	84.5	0.5	Liquid	Clear
24	98.1	99.4	0.6	85.8	0.5	Liquid	Clear
36	97.2	99.3	0.7	85.3	0.6	Liquid	Light yellow
48	97.6	99.2	0.8	85.7	0.7	Liquid	Light yellow
60	97.3	99.2	0.8	81.4	0.6	Liquid	Light yellow
72	97.6	99.2	0.8	82.0	0.6	Liquid	Yellow
84	88.8	99.4	0.6	79.6	0.5	Liquid	Light brown
96	81.3	99.5	0.5	74.4	0.3	Liquid	Light brown
102	81.4	99.6	0.4	68.5	0.3	Liquid	Light brown

จุฬาลงกรณ์มหาวิทยาลัย
Chulalongkorn University

Table B.7 Effect of time on stream for CoMoN/Al catalyst on conversion, selectivity, yield, product phase and product color.

Time on stream (h)	Conversion (%)	Selectivity (%)		Yield (%)		Product phase	Product color
		Diesel selectivity	Gasoline selectivity	Diesel yield	Gasoline yield		
1	96.2	96.2	3.8	83.7	3.3	Liquid	Clear
3	95.8	99.1	0.9	82.7	0.8	Liquid	Clear
6	96.5	98.8	1.2	81.6	0.9	Liquid	Clear
12	95.4	99.2	0.8	76.2	0.6	Liquid	Light yellow
15	94.0	98.8	1.2	67.8	0.8	Liquid	Yellow
18	85.3	99.3	0.7	65.7	0.4	Liquid	Yellow
24	79.2	99.2	0.8	66.4	0.5	Liquid	Yellow
30	79.5	98.8	1.2	62.9	0.8	Liquid	Yellow
36	77.9	99.0	1.0	61.5	0.6	Solid+Liquid	Light brown
42	71.5	97.6	2.4	41.1	1.0	Solid+Liquid	Light brown

จุฬาลงกรณ์มหาวิทยาลัย
Chulalongkorn University

APPENDIX C
CONDITION OF GAS CHROMATROGRAPY AND CALIBRATION CURVES OF STANDARDS

Table C.1 Components of n-C_5 to n-C_{44} alkanes in calibration mixture. (Songphon 2011).

Elution order	Compound	CAS#	Percent Purity	Concentration (wt.%)
1	n-Pentane (C_5)	109-66-0	99%	0.9995 wt./wt.%
2	n-Hexane (C_6)	110-54-3	99%	0.9995 wt./wt.%
3	n-Heptane (C_7)	142-82-5	99%	0.9995 wt./wt.%
4	n-Octane (C_8)	111-65-9	99%	0.9995 wt./wt.%
5	n-Nonane (C_9)	111-84-2	99%	0.9995 wt./wt.%
6	n-Decane (C_{10})	124-18-5	99%	0.9995 wt./wt.%
7	n-Undecane (C_{11})	1120-21-4	99%	0.9995 wt./wt.%
8	n-Dodecane (C_{12})	112-40-3	99%	0.9995 wt./wt.%
9	n-Tetradecane (C_{14})	629-59-4	99%	0.9995 wt./wt.%
10	n-Pentadecane (C_{15})	629-62-9	99%	0.9995 wt./wt.%
11	n-Hexadecane (C_{16})	544-76-3	99%	0.9995 wt./wt.%
12	n-Heptadecane (C_{17})	629-78-7	99%	0.9995 wt./wt.%
13	n-Octadecane (C_{18})	593-45-3	99%	0.9995 wt./wt.%
14	n-Eicosane (C_{20})	112-95-8	99%	0.9995 wt./wt.%
15	n-Tetracosane (C_{24})	646-31-1	99%	0.9995 wt./wt.%
16	n-Octacosane (C_{28})	630-02-4	99%	0.9995 wt./wt.%
17	n-Dotriacontane (C_{32})	544-85-4	98%	0.9991 wt./wt.%
18	n-Hexatriacontane (C_{36})	630-06-8	99%	0.9995 wt./wt.%
19	n-Tetracontane (C_{40})	4181-95-7	97%	0.9986 wt./wt.%
20	n-Tetracontane (C_{44})	7098-22-8	99%	0.9995 wt./wt.%
Solvent	Carbon Disulfide	75-15-0	99%	

จุฬาลงกรณ์มหาวิทยาลัย
Chulalongkorn University

Table C.2 Condition of GC-FID for calibration curve.

Condition	Value
Air (kPa)	50
H_2 (kPa)	80
Carrier (kPa)	40
Make up (kPa)	40
Split (ml min^{-1})	30
Purge (ml min^{-1})	4

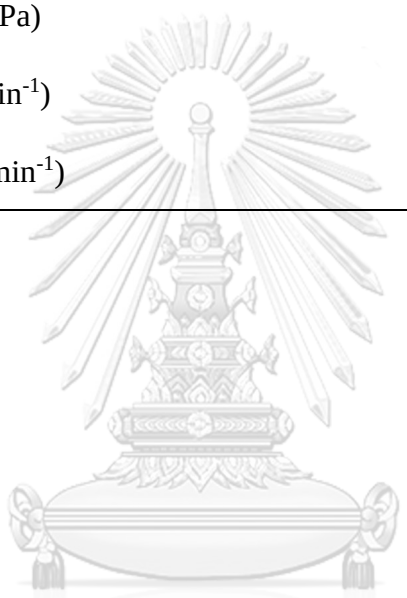

จุฬาลงกรณ์มหาวิทยาลัย
CHULALONGKORN UNIVERSITY

Table C.3 Retention time for each hydrocarbon component in calibration mixture.

Components	Retention time (Average)
n-Pentane (C5)	0.25
n-Hexane (C6)	0.45
n-Heptane (C7)	0.87
n-Octane (C8)	1.58
n-Nonane (C9)	2.53
n-Decane (C10)	3.6
n-Undecane (C11)	4.69
n-Dodecane (C12)	5.74
n-Tetradecane (C14)	7.71
n-Pentadecane (C15)	8.61
n-Hexadecane (C16)	9.45
n-Heptadecane (C17)	10.26
n-Octadecane (C18)	11.02
n-Eicosane (C20)	12.43
n-Tetracosane (C24)	14.88
n-Octacosane (C28)	16.96
n-Dotriacontane (C32)	18.76
n-Hexatriacontane (C36)	20.32
n-Tetracontane (C40)	21.98

จุฬาลงกรณ์มหาวิทยาลัย
Chulalongkorn University

Table C.4 Density and molecular weight for component in calibration mixture. (Songphon 2011)

Component	Density (g/cm^3)	Molecular weight (g/mol)
n-Pentane (C5)	0.626	72.15
n-Hexane (C6)	0.659	86.18
n-Heptane (C7)	0.684	100.20
n-Octane (C8)	0.703	114.23
n-Nonane (C9)	0.718	128.26
n-Decane (C10)	0.730	142.28
n-Undecane (C11)	0.740	156.31
n-Dodecane (C12)	0749	170.33
n-Tetradecane (C14)	0.763	198.39
n-Pentadecane (C15)	0.769	212.42
n-Hexadecane (C16)	0.773	226.44
n-Heptadecane (C17)	0.777	240.47
n-Octadecane (C18)	0.777	254.5
n-Eicosane (C20)	0.789	282.55
n-Tetracosane (C24)	0.797	338.66
n-Octacosane (C28)	0.8067	394.76
n-Dotriacontane (C32)	0.812	450.87
n-Hexatriacontane (C36)	0.7795	506.97
n-Tetracontane (C40)	0.7785	563.08
n-Tetracontane (C44)	0.82	
Carbon Disulfide	1.261	76.139

จุฬาลงกรณ์มหาวิทยาลัย
Chulalongkorn University

Calibration curve for gaseous product

Table C.5 Calibration curve for hydrogen gas**.**

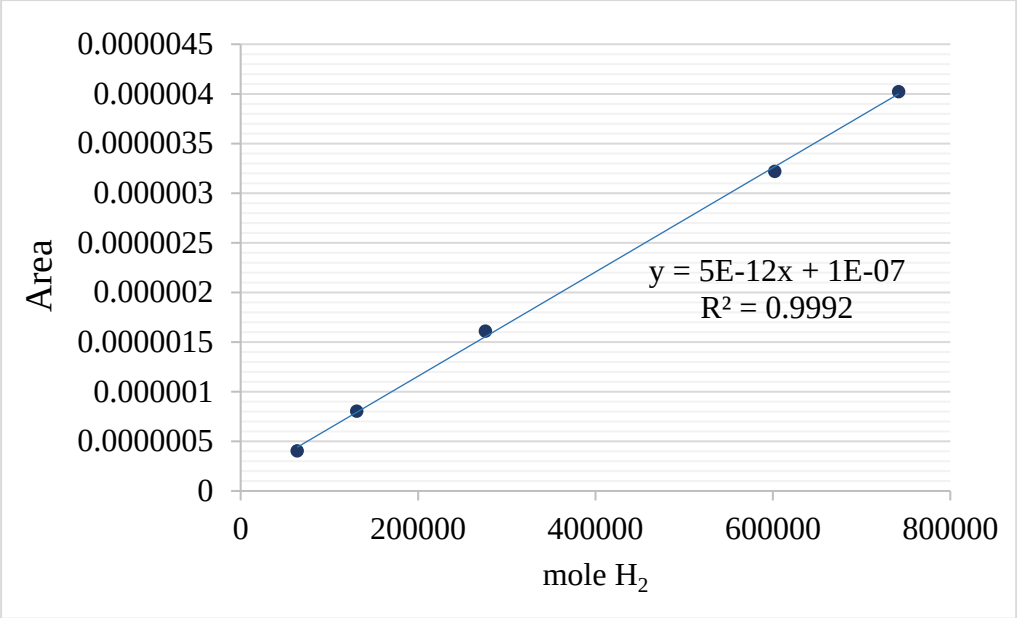

Table C.6 Calibration curve for carbon monoxide gas**.**

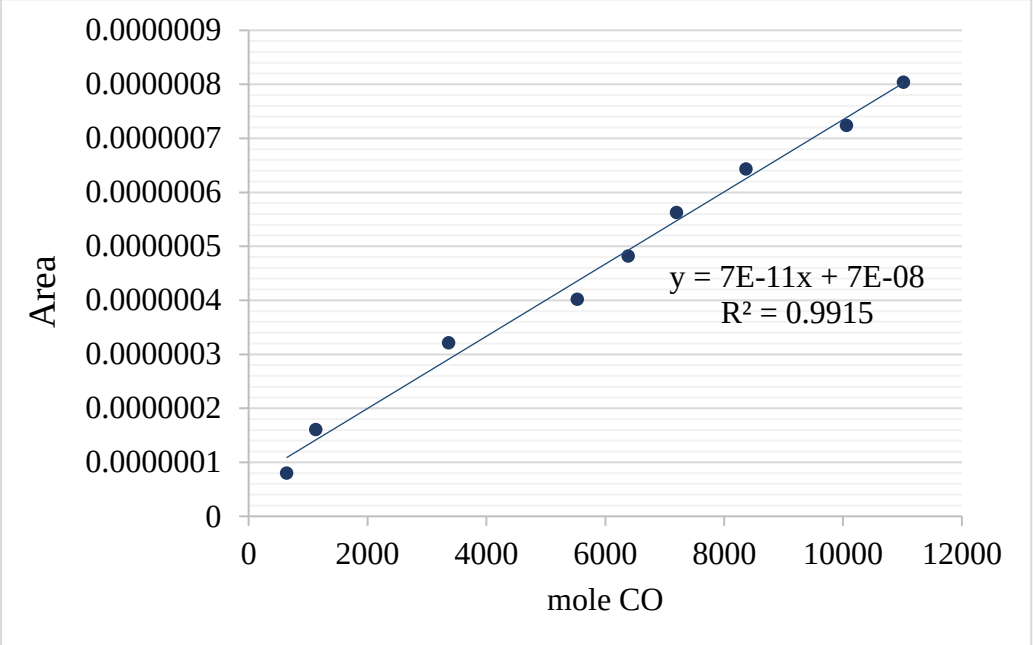

Table C.7 Calibration curve for methane gas**.**

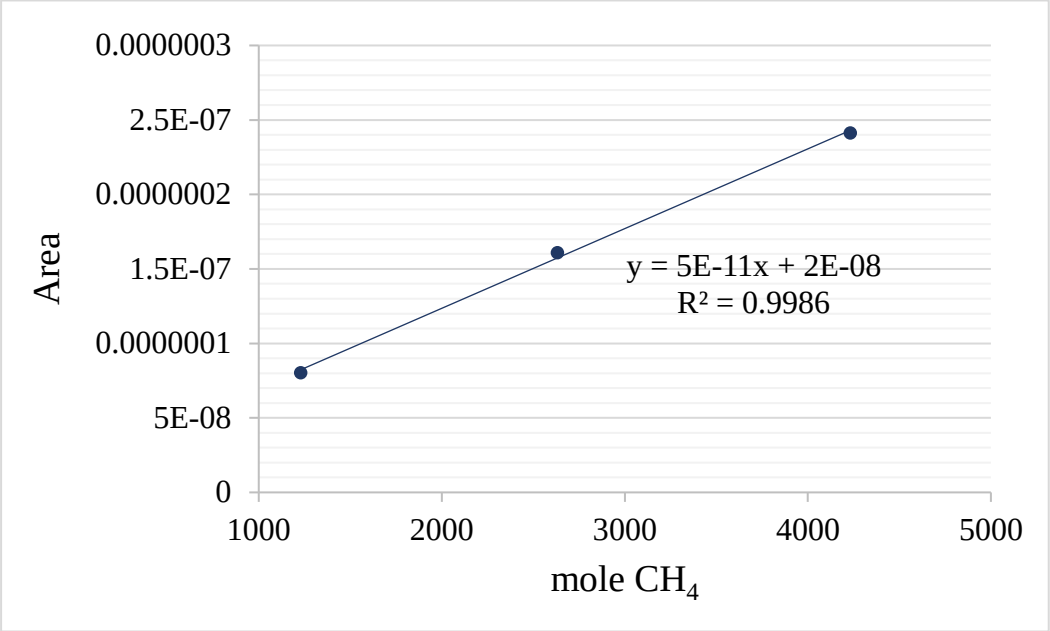

Table C.8 Calibration curve for carbon dioxide gas**.**

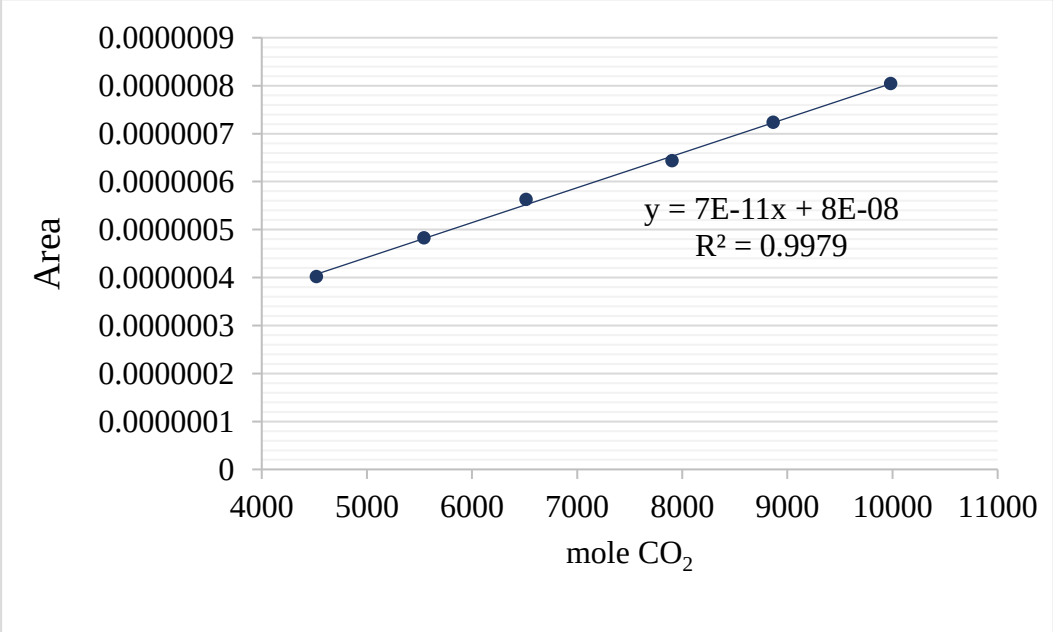

VITA

NAME	wanwipa leangsiri
DATE OF BIRTH	10 July 2538
PLACE OF BIRTH	Chachoengsao, Thailand
INSTITUTIONS ATTENDED	Center of Excellence in Catalysis and Catalytic Reaction Engineering, Department of Chemical Engineering, Faculty of Engineering, Chulalongkorn University, Bangkok 10330, Thailand
HOME ADDRESS	98/100 M.5 Pong, Banglamung, Chonburi, Thailand 20150

จุฬาลงกรณ์มหาวิทยาลัย
CHULALONGKORN UNIVERSITY